Effect of Volume Fraction on Shear Mode Properties of Co-Fe and Ni-Fe Filled Magneto-Rheological Elastomers

By

Shayan Tahir

(Registration No: 273450)

Department of Structural Engineering

School of Civil and Environmental Engineering

National University of Sciences & Technology (NUST)

Islamabad, Pakistan

(2022)

Effect of Volume Fraction on Shear Mode Properties of Co-Fe and Ni-Fe Filled Magneto-Rheological Elastomers

By

Shayan Tahir

(Registration No: NUST273450)

A thesis submitted to the National University of Sciences and Technology, Islamabad,

in partial fulfillment of the requirements for the degree of

Masters of Science in
Structural Engineering

Thesis Supervisor: Dr. Muhammad Usman

School of Civil and Environmental Engineering

National University of Sciences & Technology (NUST)

Islamabad, Pakistan

THESIS ACCEPTANCE CERTIFICATE

Certified that final copy of MS Thesis written by Ms Shayan Tahir (Registration No. 273450), of SCEE / Nust Institute of Civil Engineering has been vetted by undersigned, found complete in all respects as per NUST Statutes/ Regulations/ MS Policy, is free of plagiarism, errors, and mistakes and is accepted as partial fulfillment for award of MS degree. It is further certified that necessary amendments as point out by GEC members and foreign/ local evaluators of the scholar have also been incorporated in the said thesis.

Signature: _____

Name of Supervisor Dr. Muhammad Usman

Date: _____

Signature (HOD): _____

Date: _____

Signature (Dean/ Principal) _____

Date: _____

Attach copy of TH-4 Form

Certificate of Approval

This is to certify that the research work presented in this thesis, entitled "……
……..……"
was conducted by Mr./Ms…… under the supervision of
…….. .
No part of this thesis has been submitted anywhere else for any other degree. This thesis is submitted to the..... (Name of Department of the University) ..... in partial fulfillment of the requirements for the degree of Doctor of Philosophy in Field of ……(Subject Name)…….
Department of ……...
University of …….

Student Name:_____ Signature:_____

Examination Committee:

a) External Examiner 1: Name Signature:_____
(Designation & Office Address)
……
……

b) External Examiner 2: Name Signature:_____
(Designation & Office Address)
……
……

c) External Examiner: Name Signature:_____
(Designation & Office Address)
……
……

Supervisor Name: Signature: _____

Name of Dean/HOD: Signature: _____

Author's Declaration

I Shayan Tahir hereby state that my MS thesis titled Effect of volume fraction on the shear mode properties of Co-Fe and Ni-Fe filled Magneto-rheological Elastomers (MREs) is my own work and has not been submitted by me for taking any degree fromthis University National University of Science and Technology H-12, Islamabad or anywhere else in the country/ world.

At any time if my statement is found to be incorrect even after I graduate, the university has the right to withdraw my MS degree.

Name of Student: Shayan Tahir

Date: _____

Plagiarism Undertaking

I solemnly declare that research work presented in the thesis titled "Effect of volume fraction on shear mode properties of Co-Fe and Ni-Fe filled Magneto-rheological Elastomers (MREs)" is solely my research work with no significant contribution from any other person. Small contribution/ help wherever taken has been duly acknowledged and that complete thesis has been written by me.

I understand the zero tolerance policy of the HEC and University, National University of Science and Technology (NUST) H-12 Islamabad, towards plagiarism. Therefore, I as an author of the above titled thesis declare that no portion of my thesis has been plagiarized and any material used as reference is properly referred/cited.

I undertake that if I am found guilty of any formal plagiarism in the above titled thesis even after award of MS degree, the University reserves the rights to withdraw/revoke my MS degree and that HEC and the University has the right to publish my name on the HEC/University website on which names of students are placed who submitted plagiarized thesis.

Student/Author Signature: _____

Name: Shayan Tahir

Dedicated to my parents.

ACKNOWLEDGEMENTS

In the words of Ralph Waldo Emerson, “Cultivate the habit of being grateful for every good thing that comes to you, and to give thanks continuously. And because all things have contributed to your advancement, you should include all things in your gratitude”. These words portray the importance of expressing gratitude towards others. This piece of work would not have been possible without the support of several people, some of whom I’ll mention here.

First and foremost, I am thankful to Allah Almighty for showering his blessings upon me and giving me the strength to complete this task. I would also like to thank my supervisor, without whose guidance the task of understanding my path would have been very difficult. I credit his surveillance, which helped me in accomplishing this task. I am also thankful to my parents who provided me with constant support throughout this time. This research would not have been possible without them. Last but not the least, I would also like to thank my friends for moral support.

ABSTRACT

To provide adaptability to passive seismic isolation devices the magneto-rheological elastomers are used. In this research, the synergistic behavior of magnetorheological elastomers containing nickel and cobalt along with iron particles as magnetically polarizable fillers is examined experimentally under dynamic shear loading. Two different types of magnetorheological elastomer were fabricated having equal proportions of iron and nickel in one kind, and iron and cobalt in the other. The concentrations of magnetic particles in each type are varied from 10% to 40% and investigated for several frequencies, displacement amplitude, and magnetic field values. A test assembly with moveable permanent magnets was used to vary magnetic field density. Force displacement hysteresis loops were studied for the dynamic response of MREs. It was observed that MREs showed a linear behavior at low strains while nonlinearity increased with increasing strain. The percentage filler content and frequency increased the MRE stiffness whereas it decreased with displacement amplitude. The computed maximum MR effect was 55.56 percent. While MRE with iron and cobalt gave the highest effective stiffness, MRE with iron and nickel gave the highest MR effect.

Keywords: Magneto-rheological elastomers; iron; cobalt; nickel; shear mode; high strains; percentage filler content

TABLE OF CONTENTS

LIST OF TABLES

LIST OF FIGURES

LIST OF SYMBOLS, ABBREVIATIONS AND ACRONYMS

MRE	Magneto-rheological Elastomers
BI	Base Isolation
Ni-Fe	Nickel and iron particles as filler
Co-Fe	Cobalt and iron particles as filler
MR	Magneto-rheological
Keff	Effective stiffness
*f*max	Max force
*f*min	Min force
*d*max	Max displacement
*d*min	Min displacement
Keff (0T)	Effective stiffness at 0 flux
Keff (0.4T)	Effective stiffness at 0.4 flux

CHAPTER 1: INTRODUCTION

There are two methods to control the effect of vibration in a structure i.e. vibration damping and vibration isolation. Base isolation is the most common and efficient technique of vibration isolation of a structure. With innovation in materials and techniques, the limitations of adaptability along with low frequency, and high amplitude performance can be improved.

1.1 Introduction

Base isolation history dates back to 19th century. It has been extensively used over the last decades for the seismic protection of buildings and bridges [1]. Passive base isolation (PBI) installed in buildings not only suppresses vibrations, but also ensures safe use of the buildings after earthquakes [2]. These systems decouple the components of building from direct contact with the horizontal displacements of the ground so, the transmission of vibration to the primary structure is reduced [3,4]. Horizontally flexible devices are used which possess sufficient vertical rigidity to ensure stability and to limit vertical deformations, and high horizontal flexibility to allow displacements during seismic event to occur at system isolation level [5]. Thus, significantly decreases the relative displacements and absolute acceleration of the structure [2].

The mechanism of an isolation system is explained as follows, by providing the flexibility of the support the natural period of the structure can be increased [6] this elongation of natural period helps in shifting the fundamental frequency of the structure away from the dominant frequencies of the ground motion [7]. Hence, protecting it

against detrimental effects due to resonance of structure [8]. This technique also provides energy dissipation to reduce the force demands so that the relative displacements are controlled [6]. Base isolation provides (ample) rigidity against unnecessary motions due to wind or other ambient vibrations [1] and enables the designers to adjust damping and structural periods [8]

Base isolation has limitation in its use in low frequency ground motions and once installed its properties cannot be altered. To provide adaptability to a passive base isolator smart materials like magnetorheological elastomers are used [9,10]. Base isolators with MRE layers are shown in ***Figure 1.1***. MREs can undergo raid and reversible stiffness and damping changes in the presence of magnetic field [11]. they consist of polarizable particles embedded in rubber matrix. Upon application of magnetic field, the attraction between the particles grows and they align themselves in chains which results in stiffness changes of elastomers [12,13]. The properties of the elastomers are highly affected by filler type, shape, size, and percentages added.

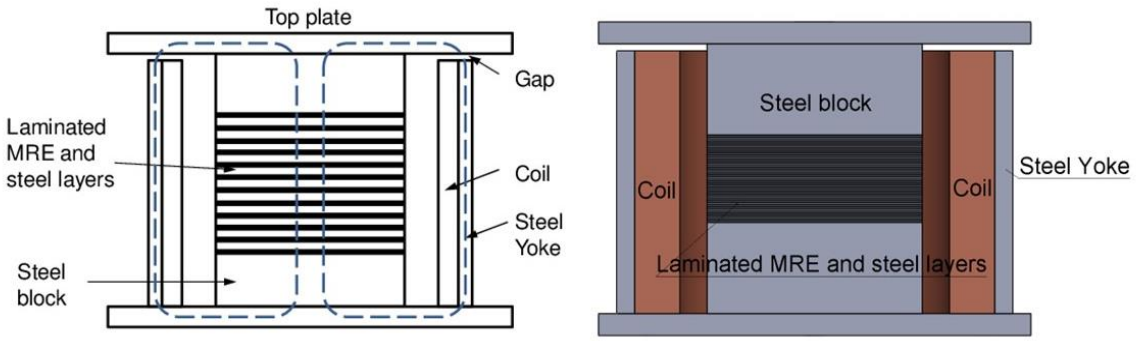

Figure 1.1 Base isolators with magneto-rheological elastomer (MRE) layers [14,15]

Although used by many researchers' iron particles are difficult to handle while casting due to their corrosive nature and poor oxidative stability. Cobalt and nickel

particles have also been extensively used in recent years either in their pure form or in the form of their ferrites. They have excellent properties like oxidization stability, good corrosion resistance and electrical properties. Two increase their MR effect iron particles are added with them. The dynamic properties of magnetic particles have been studied in detail at high frequencies and amplitude.

1.2 Problem Statement

To target a filler material that does not oxidize easily, have better corrosion resistance and more MR effect.

MREs with cobalt and nickel as fillers provide resistance to oxidization and corrosion along with good electrical properties but their MR effect is considerably reduced. Hence this research aimed at the improvement of MR effect of MREs incorporated with Co and Ni particles by adding iron particles with them.

1.3 Objectives

- To fabricate magneto rheological elastomers using nickel and cobalt particles along with iron particles as polarizable filler.
- To study different composition ratios of these hybrid fillers at large strains under shear loading (and compare their dynamic properties.
- To study the magneto rheological properties/performance of Co-Fe and Ni-Fe MREs.)
- To study and compare the dynamic and magneto rheological properties of Co-Fe and Ni-Fe MREs.

1.4 Research Significance

A lot of research has been carried out to develop Magneto rheological Elastomers using cobalt and nickel as magnetizable filler particles. They added to the MREs in their pure form and in the form of their ferrites. Several tests are performed to evaluate their dynamic properties. The effect of their shape morphology and size on mechanical properties is also studied. However, those researches lack the study of varying filler percentages of cobalt and nickel particles in MREs, along with their performance at low frequencies and high amplitudes. Also, the magnetic rheological properties of these MREs are affected. This research aims to perform a detailed study on the effect of their volumetric concentrations on dynamic properties and increasing their MR effect.

1.5 Research Scope

- To increase MR effect by adding iron particles with nickel and with cobalt particles.
- MREs with filler percentages of 10, 20, 30, and 40 % by volume of elastomer are fabricated.
- Shear mode dynamic tests are performed for the test parameter of 0.5, 1, 2, 3, and 5 Hz frequencies, 4.2, 7, and 9.8 mm displacement amplitude and 0, 0.1, 0.2, 0.3 and 0.4 Tesla magnetic field.
- Dynamic and MR properties are evaluated and compared for nickel-iron and cobalt-iron composites of MREs, and conclusions are drawn.

1.6 Relevance to national needs

Pakistan lies on the boundary of three interacting tectonic plates i.e., Eurasian,

Arabian and Indian plates, which makes it highly susceptible to earthquakes. Looking at the historical patterns of damage that they caused, there is a need to achieve seismic resilience in Pakistan. Base isolation is an effective seismic protection technique that has been used for decades to minimize loss of lives and infrastructure as it surpasses ground motion vibrations caused by earthquakes.

Base isolation is a passive technique as it is not capable to handle varying frequencies. To enhance versatility; MRE's has been introduced to the base isolation technique. MRE's are smart materials that provide varying stiffness and damping on the application of magnetic field which makes them adaptable to wide range of frequencies. Innovation and improvement in MR fillers help us improve the properties of MRE's to achieve desired results.

1.7 Thesis organization

Chapter 1 describes the background of the work with a brief introduction of base isolators and magnetorheological elastomers (MREs). It includes the hypothesis and objectives we aim to achieve with this research. It also explains the significance of the work performed and its relevance to our national needs. The scope of work is defined, and its advantages are discussed. Further, the applications of this research and the use of MREs in various devices are also discussed.

Chapter 2 contains a literature review explaining MREs in detail and the effect of their components on mechanical properties. It discusses the filler particles used in MREs and previous works on cobalt and nickel particles as polarizable fillers, their test parameters, and their properties.

Chapter 3 is the discussion of materials and methods used in this research. It

contains the description of the procurement of materials, calculations for proportions used, and the procedure applied for the casting of MREs.

Chapter 4 is about experimental investigations. The material characterization tests are discussed, and dynamic test parameters and mechanism is explained.

Chapter 5 discusses the results obtained from dynamic testing. It elaborates the effect of each parameter on the MRE properties. Results are presented and discussed in both tabular and graphical form. Hysteresis loops and stiffness graphs are discussed along with MR effect.

Lastly in chapter 6 conclusions are drawn and recommendations are given for further research. Also references for research are added in bibliography at end.

CHAPTER 2: LITERATRE REVIEW

Magneto-rheological (MR) phenomenon was invented back in the late 1940s and because of the intelligent nature and functionality of MR materials; investigations on the material, fabrication, characterization and dynamic properties are still ongoing [16,17]. The most renowned MR materials include MR fluids, MR elastomers, MR grease, and MR foams. Magnetorheological Elastomers (MREs) are one of these smart materials which when subject to an external magnetic field tend to change their mechanical and rheological properties such as stiffness, natural frequency, and damping capacity [18–21]. The controllability of mechanical and rheological properties of MRE makes them resilient over a wide range of disturbance frequencies [22,23]. MRE might have a slower response as compared to Magnetorheological Fluids depending on the type of matrix used, but they do offer more manageable rapid and reversible changes in stiffness as well as damping [16,24]. They also have the additional benefits of less sedimentation and leakage issues as compared to MR fluids [25,26].

2.1 Composition of MREs

The composition of MREs usually contains a non-polarizable solid-state viscous material for matrix, polarizable filler material for MR effect, and additives to gain certain properties [18,24,27]. MREs are fabricated by mixing the desired percentages of ferromagnetic particles in the elastomeric matrix with or without the additives. They are then cured in the presence of an external magnetic field for anisotropic MRE, having filler particles arranged in columnar chainlike structures [28,29]. And for isotropic MREs, the filler particles are homogeneously distributed in the matrix as no external magnetic field is applied [12,30]. After curing the particles are fixed in their respective

positions in a solid matrix and upon application of an external magnetic field, the particles are polarized, causing them to align themselves in chains, this is known as the MR effect [16,31,32]. This MR effect is attributed to changes in shear modulus (G), young's modulus (E), and stiffness (K) of MRE [18,19]. Which varies with the different parametric characterization of MREs such as type of matrix material, use of additives, type, percentage content, size, shape, and distribution of magnetic particles, and the external stimuli such as amplitude and direction of a magnetic field [11,33].

2.1.1 Matrix material for MREs

The carrier matrix for MREs is usually a vulcanized polymeric viscous material such as natural rubbers, vinyl rubbers, thermoplastic elastomers, silicone rubbers, and polyurethane rubbers [11,28]. When choosing a matrix for MREs softer rubbers like silicone rubbers are preferred [26] because when subjected to an external magnetic field, soft elastomeric matrixes provide less resistance against particle movement which allows particle distribution to change vastly [25]. In other words, the softer matrixes lead to a greater MR effect. Another advantage of silicone rubber is its resilience towards heat and chemical attacks [26].

2.1.2 Additives

Another optional component in MREs fabrication is additives. Additives in MR elastomers are added for several reasons like improving its mobility, softening the elastomeric matrix, and decreasing the viscosity, damping ratio, and storage modulus [22]. Silicon oil is quite commonly used as an additive in MREs for preventing agglomeration and forming a homogenous filler particle distribution. It also increases the MR effect by helping in forming a softer polymeric matrix [33].

2.1.3 Filler particles

The most influential component in the composition of MREs is ferromagnetic filler particles as they are responsible for the magnetic field induced response [27]. Commonly and frequently used polarizable material in the making of MREs is carbonyl iron particles (CIPs) [28,35]. The advantage of using iron is its high saturation magnetization and permeability (which represents its ease of magnetization) along with low remnant magnetization i.e., the remaining magnetic effect after the external magnetic field is removed [22,30,36]. Researchers have considered it quite suitable for MREs and a lot of studies have targeted the effect of changing the particle concentrations [24,32,37], size [19,30,38,39], shape [38,40], and distribution [12] on MREs. Having higher percentages of filler content is desirable, as the distances between particles are reduced and they become more sensitive and responsive to the applied magnetic field. The percentages of filler content, that are reported to produce positive results, ranging from 27 percent to 40 percent [13,16,30,41]. Apart from iron fillers, only a few limited choices are available for a selection of polarizable particles for MREs, and among them, cobalt, and nickel are reported to be the particles that have this potential [42]. Ni and cobalt are ferromagnetic materials which unlike iron do not easily oxidize and have corrosion resistance [43,44]. They are also used in MREs for their good electrical properties [36,45]. They have considerable literature as their use in MRE in pure form and in the form of their ferrites [36,45–47].

2.2 Testing of MREs

The vast applications of MREs in the engineering world make it necessary to obtain thorough information about the magneto-dynamic characterization of MREs [25,48]. The goal is the study of their mechanical properties under dynamic loading in

both the presence and absence of a magnetic field with varying strain amplitude and excitation frequency [38]. Several tests that can be performed based on their mode of operation and direction of the magnetic field include uniaxial and biaxial tension-compression tests and shear tests [11,31]. It is preferred to test MREs in a shear mode more specifically for their practical use in vibration absorbers and base isolators [22] as the earthquake forces tend to have a dominant effect in shear mode [30]. Schubert et al. [49] performed tests on MREs for loading conditions of uniaxial compression, uniaxial tension, and pure shear. Gordaninejad et al. [50] studied the behavior of thick MREs under static compression and double lap shear tests. Additionally, Vatandoost et al. [51], Moreno et al. [25], and Agirre-Olabide [52] studied MRE under compression mode and Dargahi et al. [22], Norouzi et al. [53], and Jung et al. [48] performed shear tests on MREs.

2.3 Advantages

Advantages of MREs:

- MREs are more stable and easier to handle than other MR materials, also they have no leakage and sedimentation issues.
- Variable stiffness and damping properties for several applications of vibration control.
- Innovation and alternate possibilities in the choice of a filler
- better and desirable control of mechanical properties by optimizing the polarizable filler in magnetorheological elastomers.
- Achieving a filler that does not easily oxidize and has corrosion resistance along

with an increased MR effect.

- Detailed analysis of performance at various volume percentages, frequencies, and high amplitudes. (Detailed behavior known for design requirements)

- Their use in base isolators for seismic protection of structures and bridges

2.4 Area of application

Magnetorheological Elastomers have several applications in

- Vibration isolation and vibration damping devices

- Adaptive stiffness devices

- Sensors

- controllable semi-active vibration control devices i.e., adaptive tuned vibration absorbers (ATVAs),

- various mechanical devices like variable damping beams and sandwich beams

- devices with the requirement of stiffness or modulus tunability

2.5 Research Gap

MREs with cobalt and nickel have relatively less MR effect so in order to enhance the magnetic properties of MRE; addition of iron particles along with nickel or cobalt particles is proposed in this study. Considering permeability of iron is higher than nickel and cobalt [40,43], mixing it with them can deliver a higher MR effect. Moreover, a detailed study of their stiffness and MR effect at different filler percentages of cobalt and nickel particles with iron in magneto-rheological elastomers needs to be explored

along with their performance at high amplitudes.

For this study, two hybrid formulations of MREs were prepared: one by adding iron and cobalt together as a filler and the other one having iron and nickel. Equal quantities of cobalt and iron powders were added for Co-Fe MREs and equal quantities of iron and nickel powders were added as a filler for Ni-Fe MREs. To make a better comparison based on the percentage filler in MREs, the varying percentages of filler material ranging from 10% to 40% by volume of MRE were studied. The dynamic behavior of MREs with hybrid filler was characterized along with its effects on stiffness and magnetization. Each elastomer was added with 10% silicone oil to improve particle dispersion and reduce the hardness of the matrix. PSA and SEM material characterization tests were carried out to investigate particle size, shape, and dispersion in the matrix. To investigate the effect of magnetic flux, frequency, and strain amplitude on the hysteresis and stiffness of MREs, a series of dynamic double lap shear tests were performed. Co-Fe MREs are reported together with Ni-Fe MREs to evaluate and compare their dynamic properties.

CHAPTER 3: EXPERIMENTAL INVESTIGATION

3.1 Materials

The components used for the fabrication of MREs were silicone rubber, silicone oil, and powders of iron, cobalt, and nickel. Silicone rubber RTV1505 produced by Shenzhen Rongxingda Polymer Material Co.Ltd was sourced from China in the form of part A Rubber and part B hardener. The values of hardness, viscosity, elongation, and tensile strength are 5 +/- 2 Shore A, 5000 +/- 500 mPas, ≥ 550% and ≥ 2.5 Mpa respectively. Silicon oil is produced and provided by Miingcheng Group Ltd. Dongguan, G Dong, China. It is used as an additive in the MRE. Iron particles in the size of 3-5 micrometers were procured by Gongyi City Meiqi Industry & Trade Co., Limited. Cobalt and nickel powders were also procured from China. The particle sizes chosen for all three fillers were in micrometers.

3.2 Material Characterization

For material characterization, several tests including PSA and SEM were performed.

3.2.1 Particle size analysis

Particle size analysis was performed for all three filler materials i.e., iron, cobalt, and nickel using Horiba Laser Scattering Particle size distribution Analyzer LA-920. This laser diffraction technique works by matching the scattering patterns i.e., the size of the sphere that scatters like the particle under test is reported. The results gave the mean diameters of iron, cobalt, and nickel to be 4.778, 7.3503, and 12.3966 micrometers. The findings revealed that iron particles are the smallest while nickel particles are the largest

in this study.

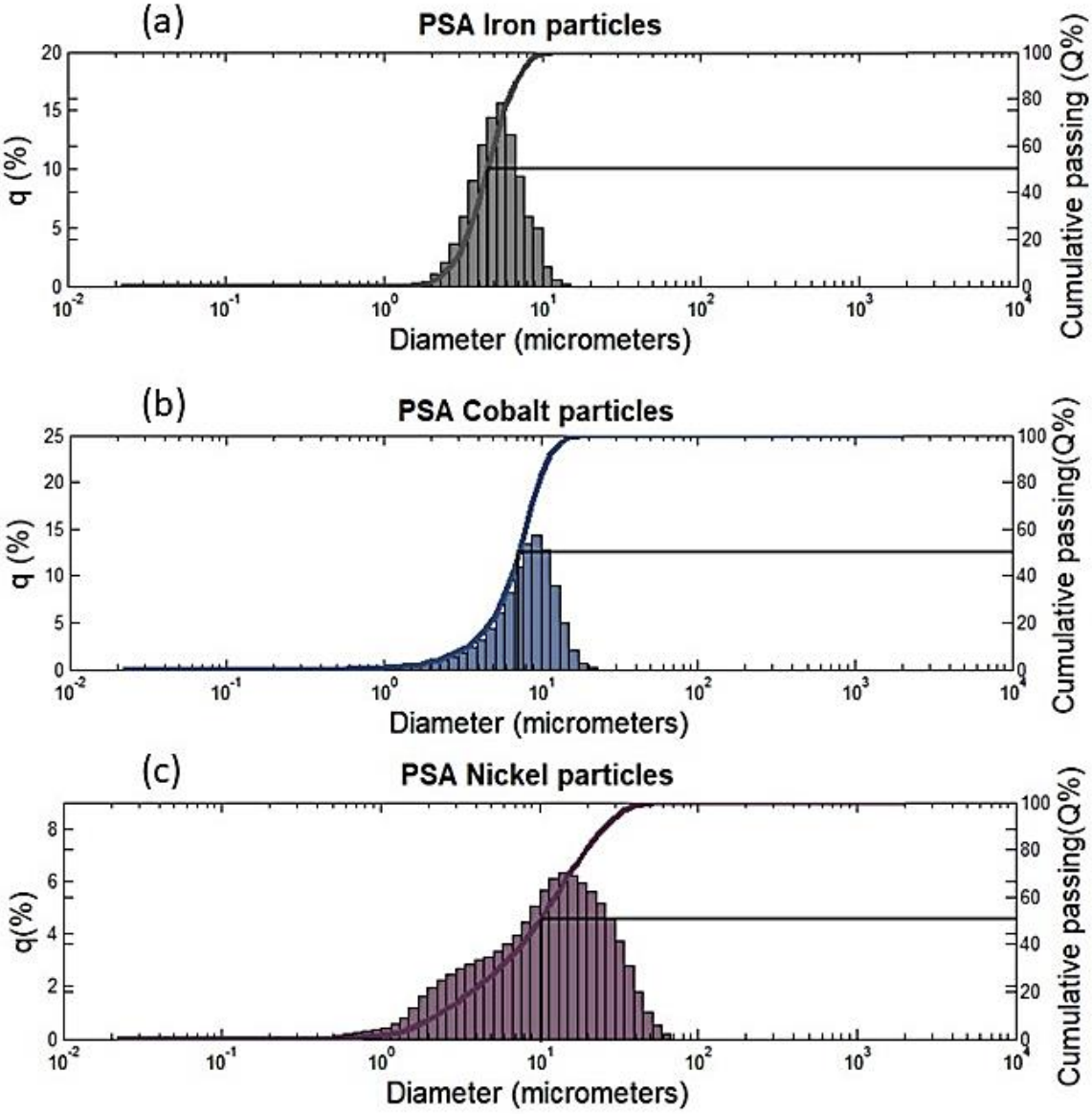

Figure 3.1 (a) Iron, (b) Cobalt, and (c) Nickel Particle size analysis (PSA)

PSA graphs for all three filler particles are plotted with cumulative passing on the y-axis and particle diameters on the x-axis. The particle size distribution is depicted in ***Figure 3.1***; the diameter value obtained by cutting the cumulative curve at 50% cumulative passing represents the median. Half of the particles in the distribution have diameters greater than this value, while the other half have diameters less than this value.

The median value observed on the graph for iron is between 4 and 5 micrometers, cobalt is be-tween 7 and 8 micrometers, and nickel is about 10 micrometers. The exact values are 4.52, 7.25, and 10.06 micrometers for iron, cobalt, and nickel respectively.

The highest peak of the histogram represents the Mode of distribution, it is the bin with the largest population of particles. In simple terms, most of the particles in the sample were of this diameter. Mode values for iron, cobalt, and nickel are 4.75, 8.21, and 12.39 respectively.

3.2.2 Scanning Electron Microscopy

Figure 3.2 shows the Scanning electron microscope (JEOL JSM-6490A) images of cobalt and nickel particles. The size and morphology of the particles are compared at 5 micrometers and 5000 magnifications. Cobalt particles can be seen to have a more defined shape than nickel particles, but both particles have irregular morphology. According to the literature these irregular morphologies of filler particles contribute to the stiffness of MREs.

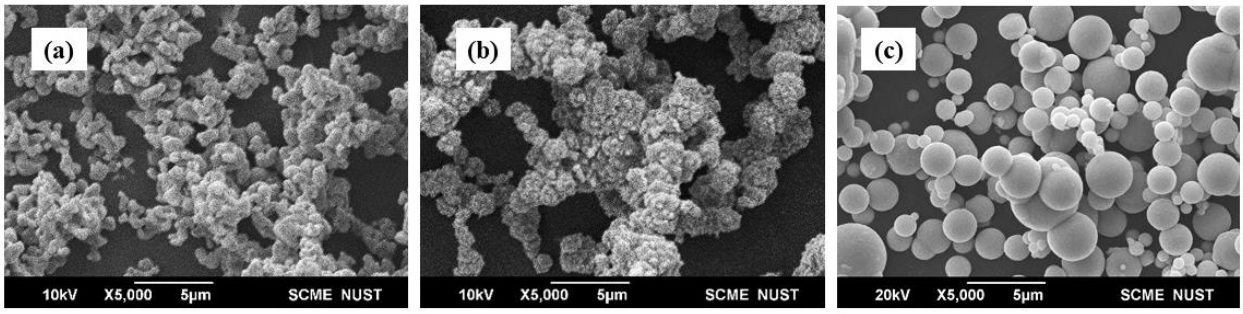

Figure 3.2 Scanning electron microscopy (SEM) images for (a) cobalt, (b) nickel and (c) iron particles

3.3 Sample preparations

For the fabrication of MREs of size 23.62x12.5x14 mm, the concentration of each component is calculated along with 15% wastage, as shown in ***Table 3.1***. Volume of

sample obtained after including the waste percentage is multiplied by percentage content of component of that specific mix to obtain the quantity of the component. Like for 80% rubber in the mix, 80% is multiplied with volume of sample including wastage to obtain the quantity of rubber, it is then converted into ml. For calculating the quantity of filler in the mix the volume including wastage is multiplied by percentage content of filler which is then multiplied by the density of the filler and divided by thousand for conversion. The apparent densities of filler particles were used which were 3.1, 1.765 and 3.2 g/cm3 for cobalt, nickel and iron particles respectively.

Table 3.1 Sample ratios and quantities

Designation	Composition	No. of Samples	% of partcicles by Vol of MREs	Filler (g) (Co-Fe or Ni -Fe)	Rubber A=B (ml)	Silicone oil by 10% vol of MRE (ml)
40% Co-Fe	Co & Fe	2	20-20	5.89-6.08	2.38	0.95
40% Ni-Fe	Ni & Fe	2	20-20	3.36-6.08	2.38	0.95
30% Co-Fe	Co & Fe	2	15-15	4.42-4.56	2.85	0.95
30% Ni-Fe	Ni & Fe	2	15-15	2.52-4.56	2.85	0.95
20% Co-Fe	Co & Fe	2	10-10	2.95-3.04	3.33	0.95
20% Ni-Fe	Ni & Fe	2	10-10	1.68-3.04	3.33	0.95
10% Co-Fe	Co & Fe	2	5-5	1.47-1.52	3.8	0.95
10% Ni-Fe	Ni & Fe	2	5-5	0.84-1.52	3.8	0.95

To acquire the desired percentage of filler in an MRE, half of the iron particles and the other half of either nickel or cobalt powder are added. The particles are measured using a sensitive weighing balance and are then mixed with part A rubber and 10% silicone oil. Using a bath sonicator of model DSA150-SK2, size: 5.7 l, the mixture is sonicated for homogeneous mixing and particle de-agglomeration. After half an hour of

sonication with intervals of hand mixing the part B rubber is added as a hardening catalyst. Rubber parts A and B are used in a one-to-one ratio. The mixture is then poured into the molds and allowed to cure for 24 hours at room temperature. Following this process, 8 pairs of MRE samples with dimensions of 23.62mm 12.5mm x 14mm were fabricated with filler percentages of 10, 20, 30, and 40%. Four of these pairings have fore mentioned concentrations of iron and cobalt as polarizable fillers, while the other four have varying quantities of iron and nickel. For instance, a 40% Co-Fe MRE was created by adding 40% filler content, which is 20% iron and 20% cobalt. Just like that if total filler content in an Ni-Fe MRE is 20 percent then it holds 10% iron and 10% nickel by volume of MRE. The quantities of filler material according to percentage content were calculated based on their apparent densities.

3.4 Sample characterization

Figure 3.3 represents the SEM images of the MR Elastomers, the overall dispersion of filler particles in the matrix can be seen. The MREs with 10% filler content are compared with the MREs with 40% particles for both Ni-Fe and Co-Fe kind.

To characterize the composition of elements in the Elastomer EDS was performed (*Figure **3.4***). The figure represents energy in KeV (kiloelectron volts) on X-axis and the peak intensity on Y-axis. The silicone peak, which is the highest, represents the elastomer's silicone matrix. The EDS of cobalt and iron shows nearly equal amounts of cobalt and iron; however, the EDS of nickel and iron shows a smaller peak than iron, which could be due to the limitations of spot analysis, x-ray overlapping or surface layer penetration.

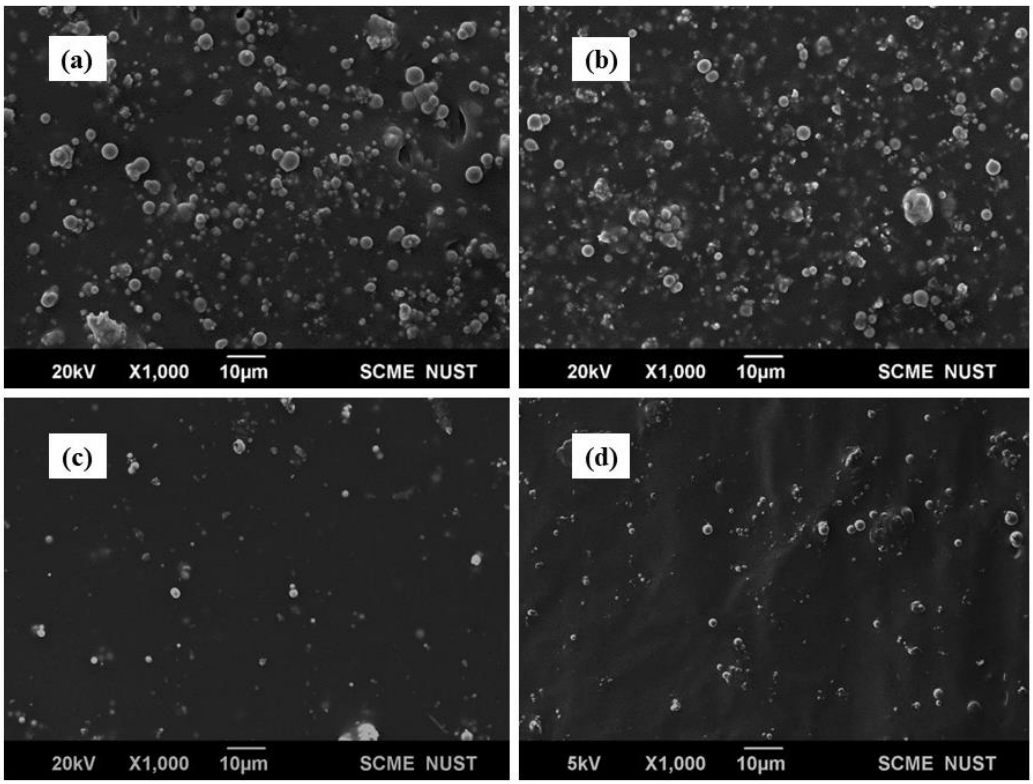

Figure 3.3 SEM images for MR Elastomers comparing 10% and 40% filler particles (a) 40% Ni-Fe (b) 40% Co-Fe (c) 10% Ni-Fe (d) 10% Co-Fe

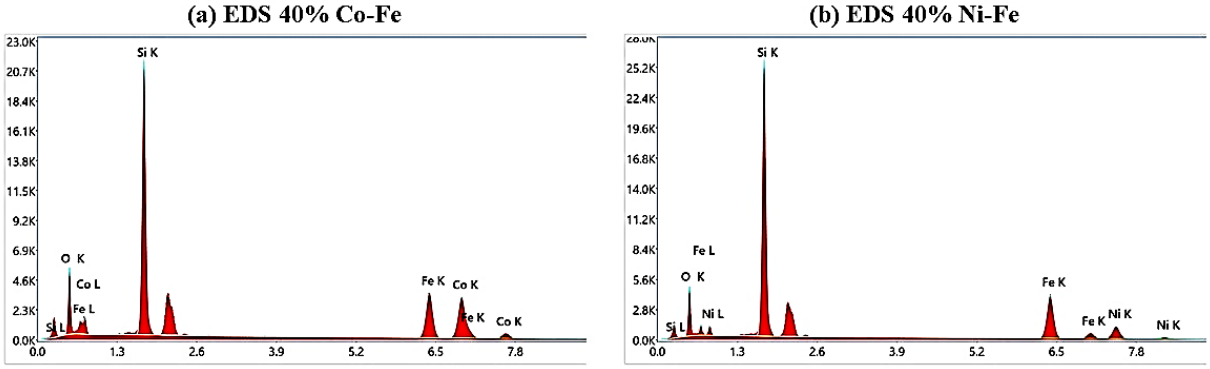

Figure 3.4 EDS (a) 40% Co-Fe (b) 40% Ni-Fe

3.5 Experimental Setup

Dynamic shear testing was performed for the mechanical properties' characterization. The same assembly was used for this study as used by Khayam et al.

[30] in their research work. The assembly consists of two grade N52 Neodymium magnets of size 50mm x 50mm x 40mm that can move forward and backward on the mild steel frame, based on the extent of the magnetic field needed. The elastomers are placed between the nonmagnetic aluminium strips with the help of superglue, the upper end of the common middle strip is attached to the machine which moves in shear during testing. A specific distance between magnets represents a specific avg flux value calculated using gauss meter and FEMM model. The assembly can provide a magnetic field of up to 0.4 Tesla. ***Figure 3.5*** represents the Finite element methods magnetics (FEMM) model used to analyze design assembly. It was designed to ensure fairly uniform flux line distribution. Also, the non-magnetic aluminum strip helps with concentrating the magnetic lines within the MRE sample.

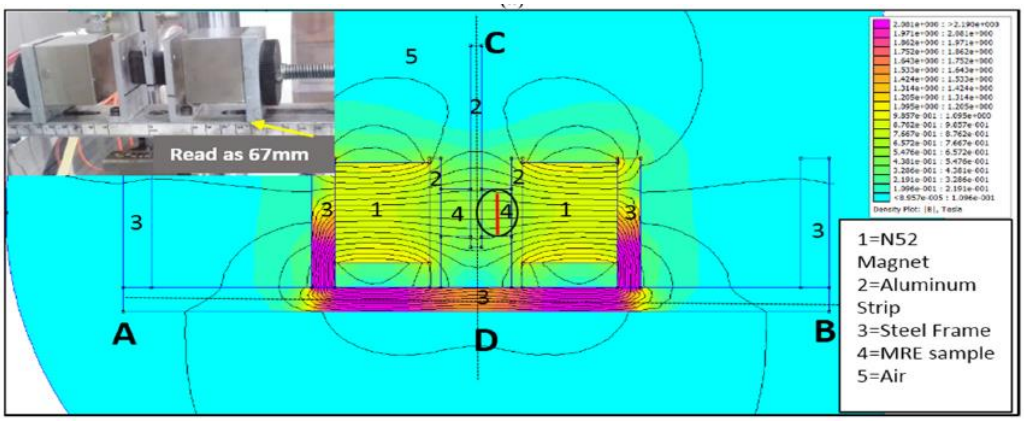

Figure 3.5 FEMM model for uniformity of flux [30]

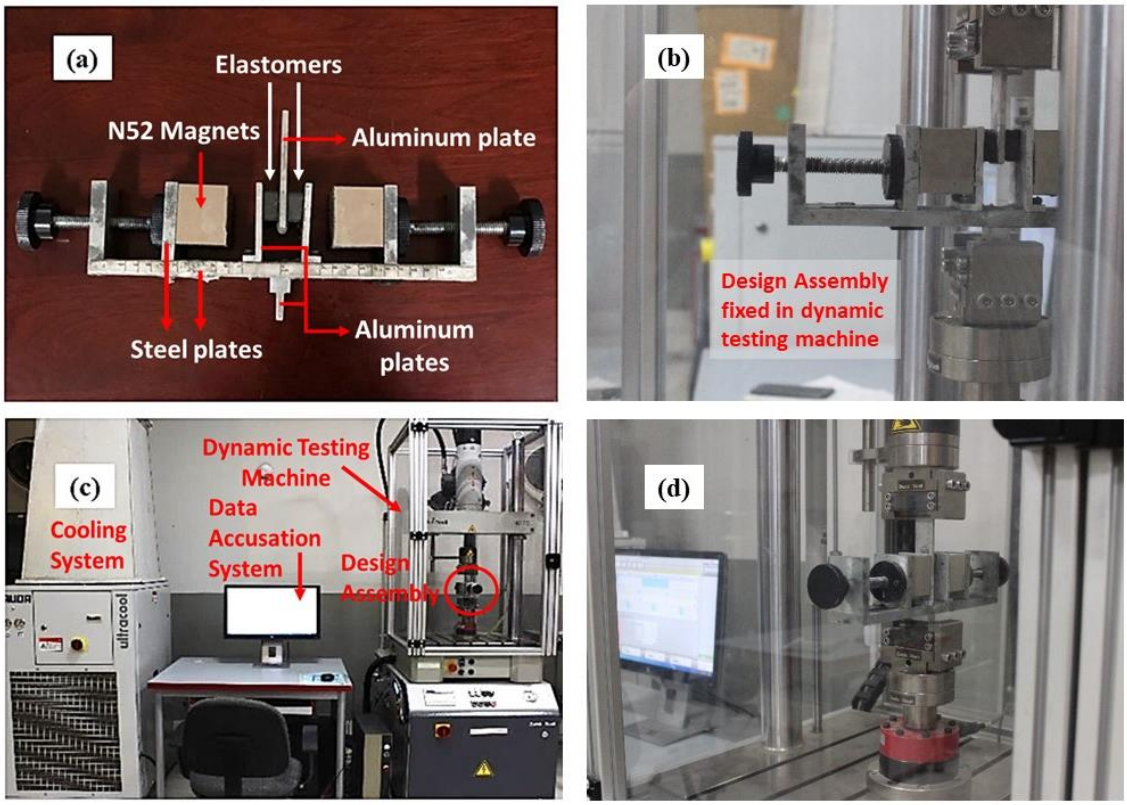

Figure 3.6 Experimental assembly and set up for dynamic testing (a) magnetic assembly holding magnets and elastomers (b), (d) experimental assembly fixated in the dynamic testing machine (c) Zwick/Roell Servohydraulic testing machine used for dynamic loading.

3.6 Dynamic Testing

Dynamic shear tests on MR Elastomers were performed using the Zwick/Roell Servo-hydraulic testing machine (HC 25) at Zwick lab in National Textile University Faisalabad, Pakistan (***Figure 3.6***c). The tests were performed for frequency values ranging from 0.5Hz, 1Hz, 2Hz, and 3Hz against displacement values of 4.2mm, 7mm, 9.8mm for 30, 50, and 70% strain. The magnetic field density was varied between values of 0T, 0.1T, 0.2T, 0.3T, and 0.4T. The test on every sample was performed for each of the frequency, amplitude, and magnetic flux values. The tests with 5Hz frequency were also performed against all magnetic flux values but only 4.2mm amplitude as the machine

cannot work for high frequencies and high amplitude simultaneously. The frequency and amplitude values are provided in the machine while magnetic flux values are changed manually by rotating the knob on the steel strips holding the magnets (***Figure 3.6***a). The flux values were calculated/confirmed using Gauss meter and were marked on the scale strip pasted on the frame below. ***Figure 3.6***b and ***Figure 3.6***d shows the magnetic assembly fixed inside the dynamic testing machine. To exterminate the Mullins's effect few cycles from the start and end of the test were eliminated from the calculation. The data for each test is acquired via the data accusation system and is stored within the system.

Table 3.2 Test parameters

Test parameters		**Cases / Variations**
% Filler content	iron + nickel	10%, 20%, 30%,40% (Each having 50% iron and 50% nickel particles)
	iron + cobalt	10%, 20%, 30%, 40% (Each having 50% iron and 50% cobalt particles)
Flux		0T, 0.1T, 0.2T, 0.3T, .4T
Frequency		0.5Hz, 1Hz, 2Hz, 3Hz, 5Hz
Disp. Amp		4.2mm (30% strain), 7mm (50% strain), 9.8mm (70% strain)

This data is extracted and filtered to remove noise and bias using Matlab software. The filtered data is then stored and used for plotting force-displacement hysteresis loops, also the effective stiffness values were calculated using this data. The formula used for effective stiffness is mentioned in equation (3.1***)***. Form effective

stiffness data the MR effect was calculated as percentage increase of effective stiffness from zero flux to maximum flux i.e. 0.4T.

$$Effective\ stiffness = Keff = \frac{f\ max - f\ min}{d\ max - d\ min} \quad \textbf{(3.1)}$$

CHAPTER 4: RESULTS AND DISSCUSSIONS

The data from the double lab shear test was utilized to investigate the dynamic characterization of MREs as well as the effect of different parameters on MRE behavior. Analyzing the obtained data revealed a considerable reliance of the hysteresis and dynamic properties on changing frequency, strain amplitude, and magnetic field density. Each of these impacts is described in greater depth in the following sections. The MREs' hysteresis and viscoelastic behavior were linked by force-displacement characterization based on experimentally collected data. The shape and slope of the hysteresis loop revealed a lot about the stiffness, damping, energy dissipation, and peak force. And all these characteristics were influenced by the changes in the displacement amplitude, strain rate, and magnetic flux.

4.1 Effect of amplitude

Figure 4.1 shows the force-displacement characteristics for the MRE containing 40% filler particles tested at different strain amplitudes for 3 Hz frequency and 0.4 T magnetic field. The slope of hysteresis loops can be seen decreasing with increasing strain amplitude, this implies that the stiffness of MREs decreases with amplitude increase as equivalent stiffness is interpreted as the slope of the major axis of the hysteresis loop [54]. Literature attributes this decrease in stiffness to Payne’s effect [42]. This strain-softening phenomenon has been frequently observed for particle-filled rubbers as the extensibility of polymer chains are affected when filler particles are present causing the bond between the rubber matrix and the filler particles to be weakened. This can also be observed by shape changes in the hysteresis loop from almost symmetrical and elliptical at low strains to non-elliptical at high amplitudes [51]. This

non-linearity and asymmetry in the force at high amplitudes is explained by the large changes produced in the spacing between the filler particles during the loading and unloading of MREs at high strains. The area of the loop also corresponds to the energy dissipation which is considered as an effect of damping implying at high amplitudes the large areas of the hysteresis loop signify more energy dissipation and damping [16].

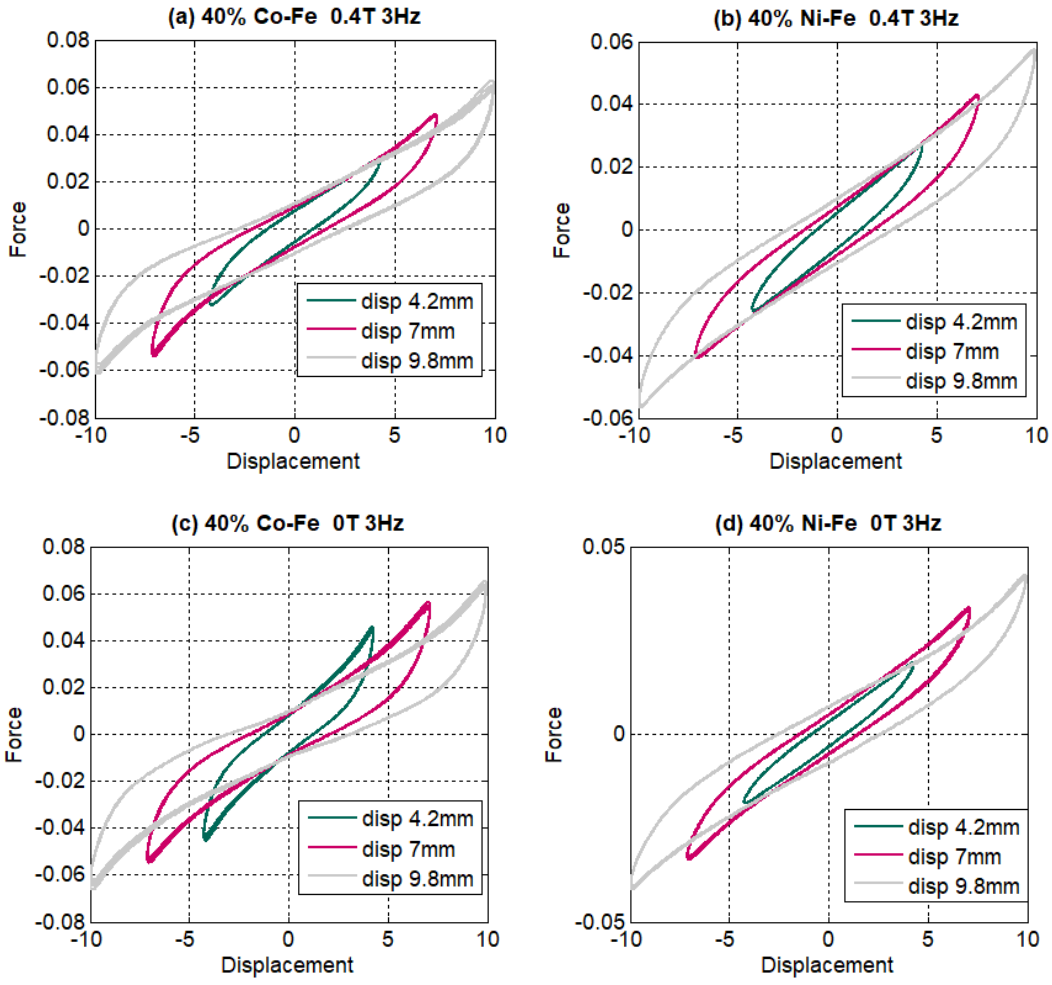

Figure 4.1 Comparison of amplitude effect on 40 % filler at maximum and minimum flux (a) 40% Co-Fe at 0.4T (b) 40% Ni-Fe at 0.4T (c) 40% Co-Fe at 0T (d) 40% Ni-Fe at 0T

Now when we compare the effect of strain amplitude with maximum and minimum magnetic field in *Figure 4.1* (b & d), the area of loop increases on the application of magnetic field offering an increase in energy dissipation with an increase in magnetic field density. The force-displacement graphs also characterize the increase in force with an increase in strain amplitude irrespective of the strain rate (frequency) and magnetic field density. The increased nonlinearity and asymmetry seen in *Figure 4.1* (c) could be because on the application of magnetic field particles interact and arrange themselves but in the absence of magnetic field there is less interaction between the particles and when strain is applied it creates more spaces between them resulting in increased nonlinearity.

For effective stiffness and amplitude graphs, the trend of mostly decreasing stiffness with amplitude can be seen ***Figure 4.2***; this trend intensifies for high filer percentages, high frequencies, and increased magnetic field.

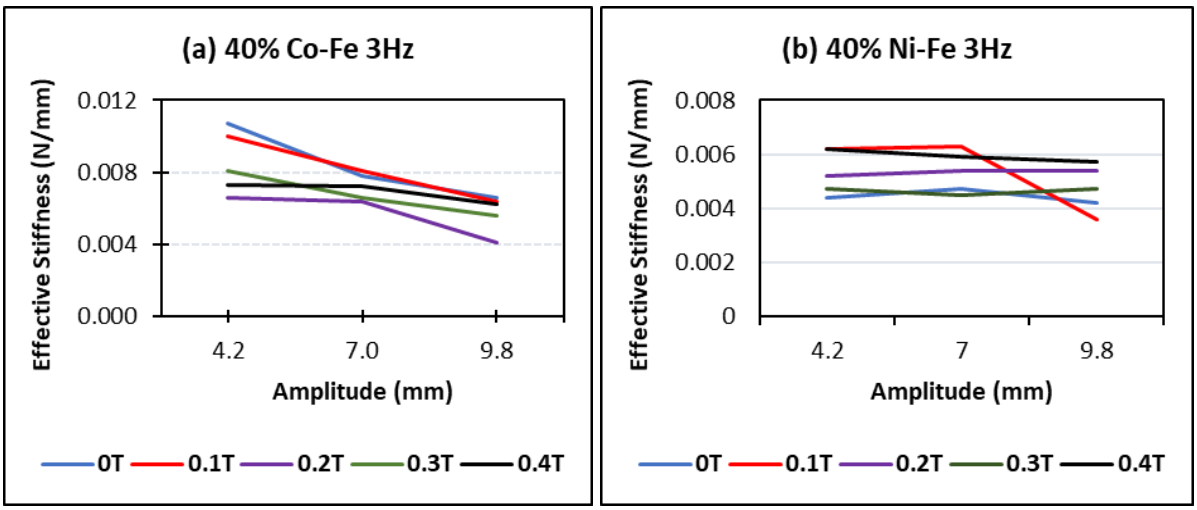

Figure 4.2 Effect of changing amplitude and flux at maximum filler and maximum frequency on the stiffness of (a) Co-Fe MRE (b) Ni-Fe MRE.

But in some cases where the values of these parameters are low, the constant stiffness can be seen and for some rare cases, it also tends to increase. This could be because of specific interactions between particles that does not break at high amplitudes. As in *Figure 4.3* (a) for a sample of higher filler content, the value of stiffness decreases with the amp at high frequency and high magnetic field going from 0.0073 to 0.0062 in the case of Co-Fe and from 0.0062 to 0.0057 in the case of Ni-Fe. But in *Figure 4.3* (b), the case of the sample with low filler content and comparatively low magnetic field the value of stiffness goes from 0.0035 to 0.0034 in the case of Co-Fe and 0.0029 to 0.003 for the Ni-Fe sample.

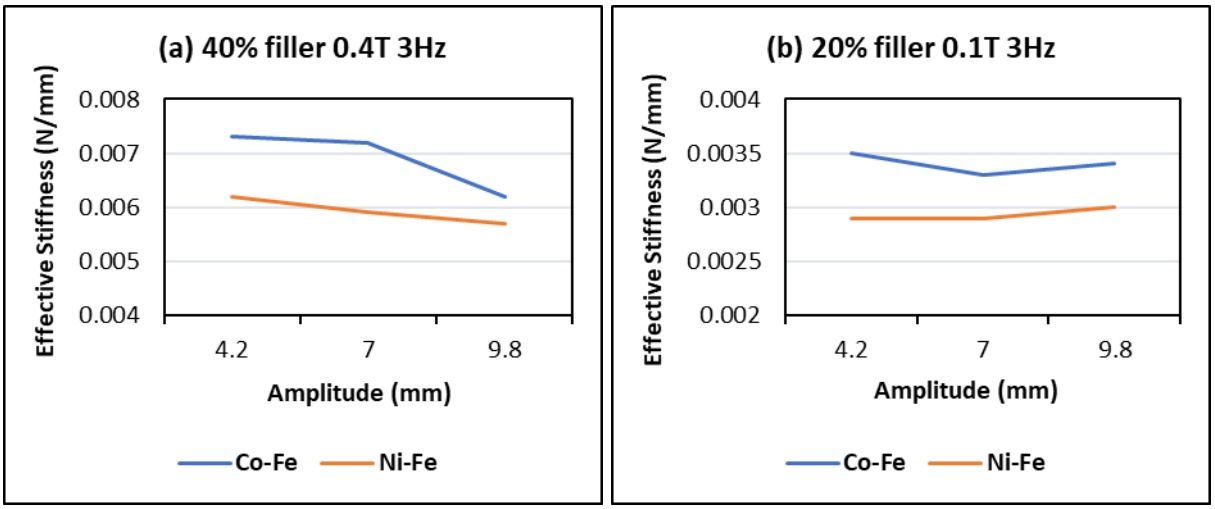

Figure 4.3 Comparison of amplitude and effective stiffness trends at (a) 40% filler and 0.4T flux (b) 20% filler and 0.1T

4.2 Effect of frequency

In *Figure 4.4* trends for different frequencies are plotted in the form of force-displacement hysteresis loops. The comparison of Ni-Fe MREs with Co-Fe MREs is made, representing the filler percentages of 40% and 10% under similar test parameters of 0.4 Tesla magnetic field and 9.8 mm displacement amplitude. The peak force is mostly

observed at maximum frequency also the trend for force increase with increasing frequency is seen. Although at higher frequencies the effect is less prominent. The wider area of the hysteresis loop indicates an increase in energy dissipation and damping at high frequencies [51]. The steeper slopes of the hysteresis loop indicate the stiffness increase. Furthermore, the graph for effective stiffness also gives a trend of increasing stiffness with in-creasing frequency. In literature, this trend is suggested as a strain rate stiffening effect [16].

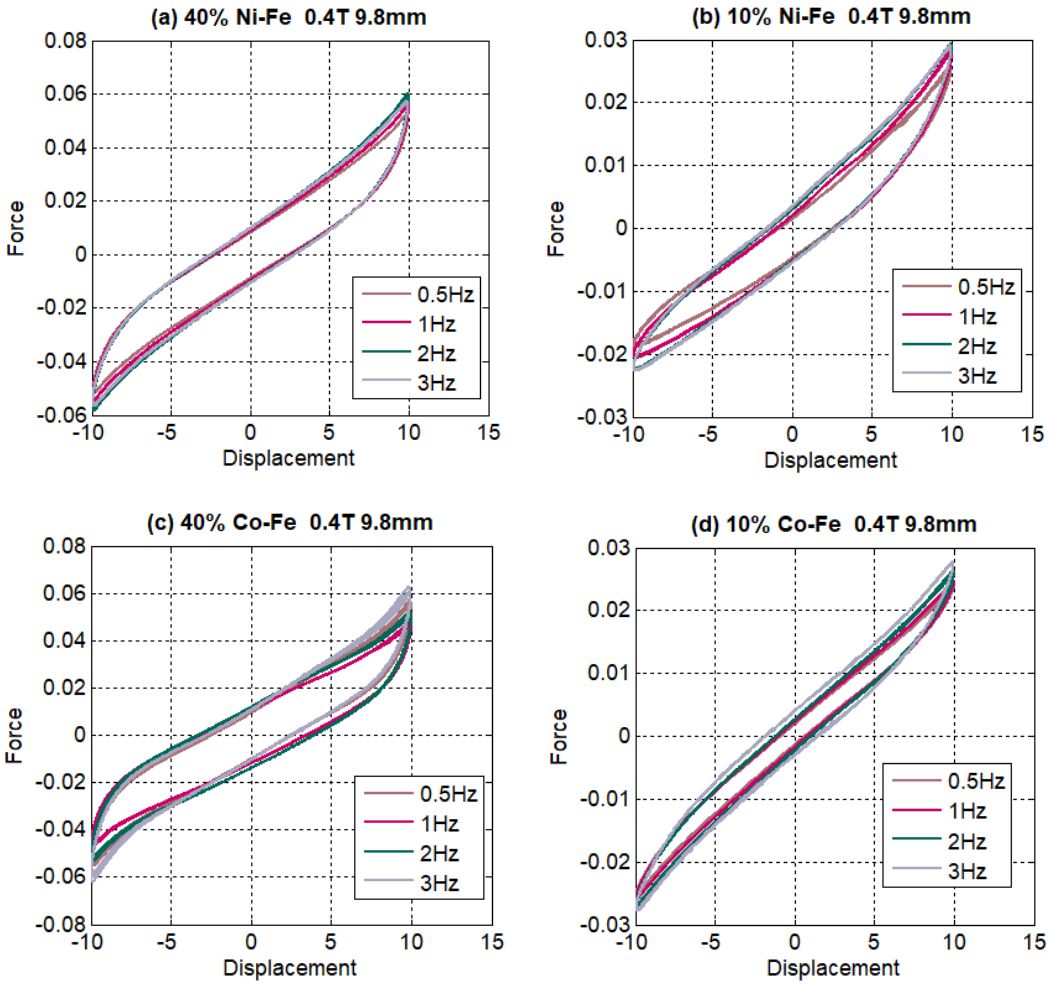

Figure 4.4 Comparison of force-displacement graphs for changing the frequency at maximum and minimum filler content for Ni-Fe MRE in (a), (b) and Co-Fe MRE in (c), (d).

Figure 4.5 represents the effect of filler percentage on stiffness increase concerning frequency and magnetic flux at a constant strain amplitude of 7 mm. The trend of gradual increase in the stiffness values can be seen going towards the higher filler percentages, as the larger percentages of filler particles contribute towards greater confinement of matrix delivering more non-linearity and stiffness. the MREs containing cobalt and iron has higher stiffness values as compared to the MREs with Nickel and iron under similar conditions. For example, in *Figure 4.5* (d) and (f) when a nickel sample gives the value of peak stiffness 0.0046 and 0.0029; the cobalt sample in *Figure 4.5* (c) and (e) for the same test conditions gives a value of 0.0051 and 0.0035 respectively. Also, 40% filler content has the highest stiffness values among the graphs in *Figure 4.5*, the maximum stiffnesses is 0.0066 for Ni-Fe and 0.0081 for Ni-Co.

This trend of stiffness increase at high frequencies is enhanced with the presence of a magnetic field, as under the influence of a stronger magnetic field attraction between the particles increases causing the matrix confinement to increase profoundly increasing force and stiffness. As it can be seen from *Figure 4.5* the most peak values of stiffness are obtained for high frequencies in the presence of high magnetic field, this effect is further discussed in the next section.

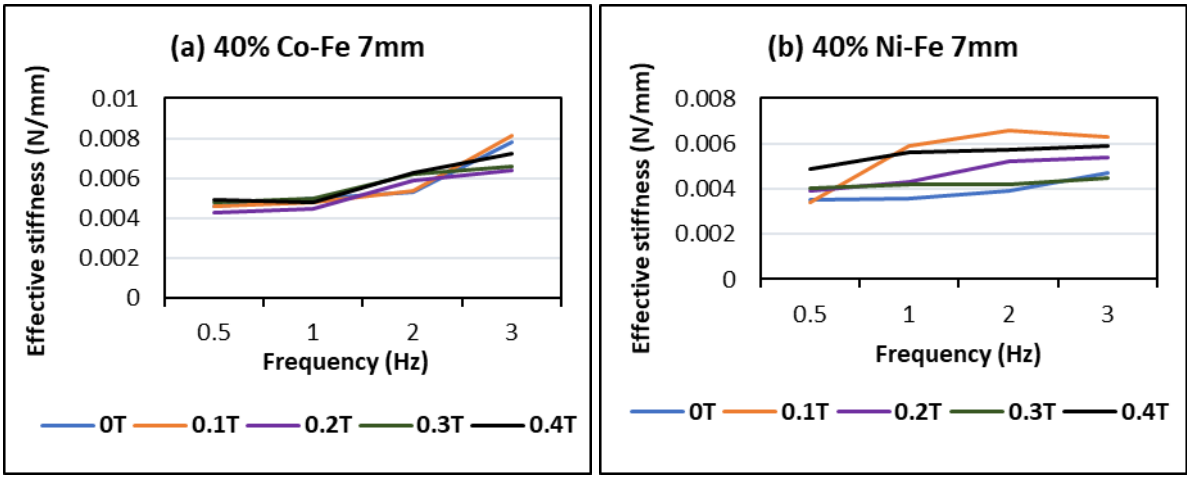

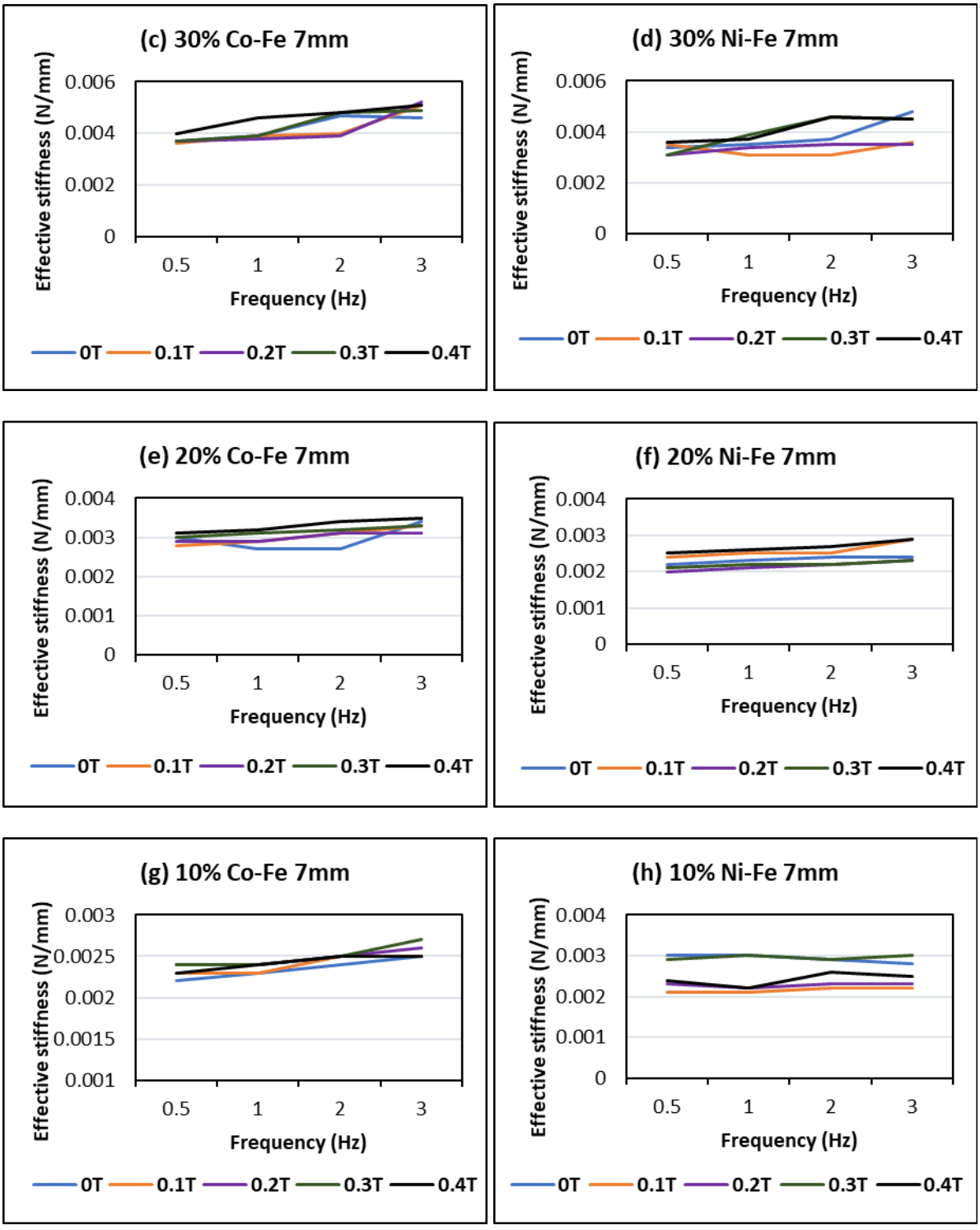

Figure 4.5 Comparison of % filler content (10, 20, 30 & 40%) between MRE containing Cobalt and Iron (a), (c), (e), (g) and MRE having Nickel and Iron (b), (d), (f), (h) while simultaneously studying the effect of frequency and magnetic field on effective stiffness

The effect of frequency and displacement amplitude on effective stiffness in *Figure 4.6* shows increase in stiffness with frequency and decrease with displacement amplitude. Thus, the highest values of stiffness are obtained for high frequency and low amplitude. This trend is more prominent in case of Co-Fe as compared to Ni-Fe.

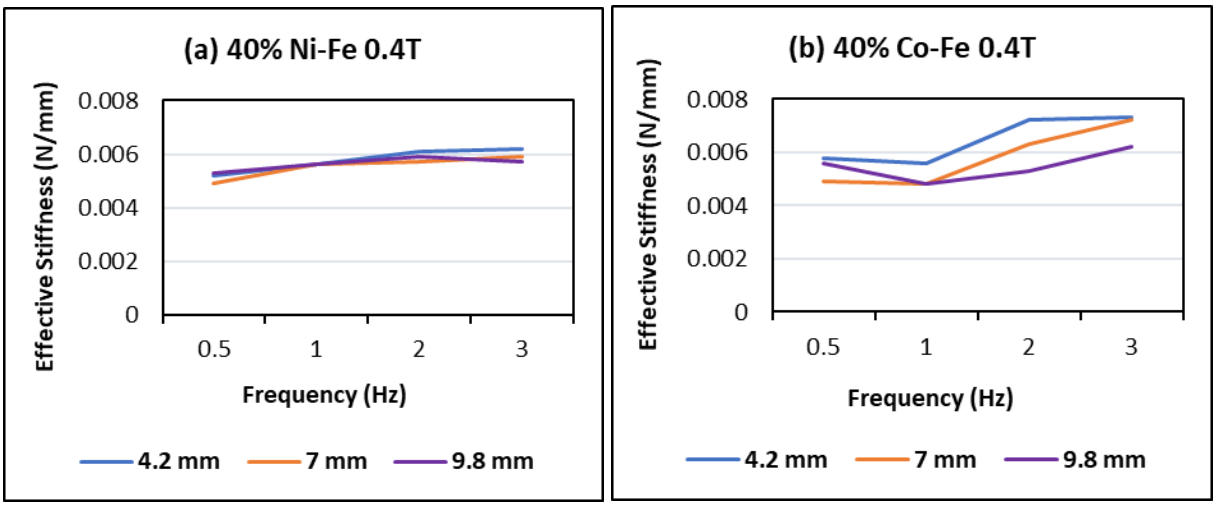

Figure 4.6 Effect of frequency and amplitude on effective stiffness at 40% filler content and 0.4T magnetic field on (a) Ni-Fe MRE and (b) Co-Fe MRE.

4.3 Effect of flux

The effect of the magnetic field is represented in *Figure 4.7* displaying hysteresis loops for 30% filler content at 3Hz frequency and 9.8mm amplitude. The trends are in correspondence with the literature where with the increase in magnetic flux the area of the hysteresis loop grows bigger and wider indicating high energy dissipation and damping [16,37,51].

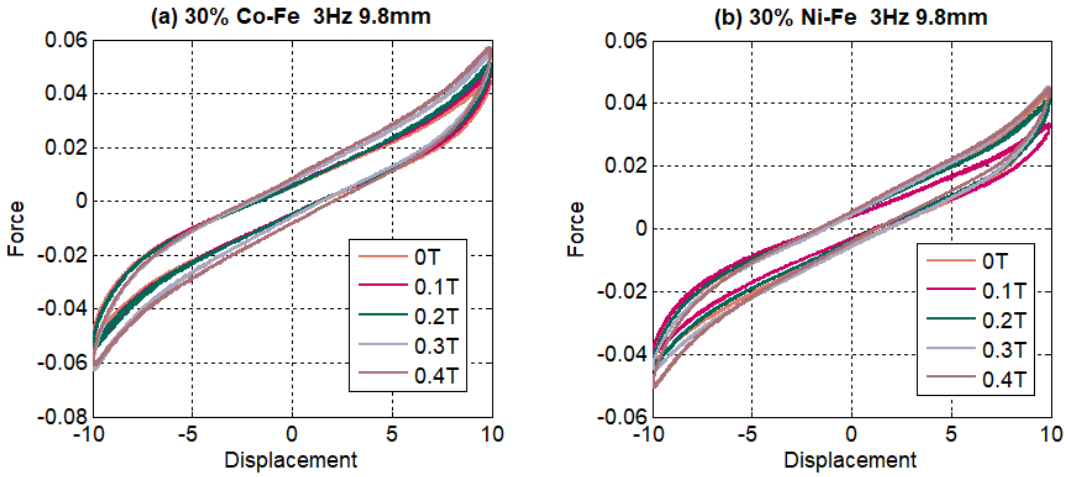

Figure 4.7 Comparison of (a) 30% Co-Fe MRE and (b) 30% Ni-Fe MRE force-displacement graphs with respect to changing flux.

Force values are also seen to be increasing going towards the high mag field density and this trend is uniform throughout the samples even though force values for iron-cobalt are higher than those for iron-nickel at the same parameters. The slopes in the force-displacement graph tend to get steeper with the growing magnitude of magnetic flux indicating stiffness increase.

The effective stiffness graphs also portray this trend of stiffness increase with flux magnitude and though a few outliners can also be seen. In *Figure 4.8* maximum stiffness values of 0.0048 and 0.0059 can be seen at the highest frequency of 3 Hz. and highest applied magnetic field of 0.4 Tesla for Co-Fe and Ni-Fe samples respectively.

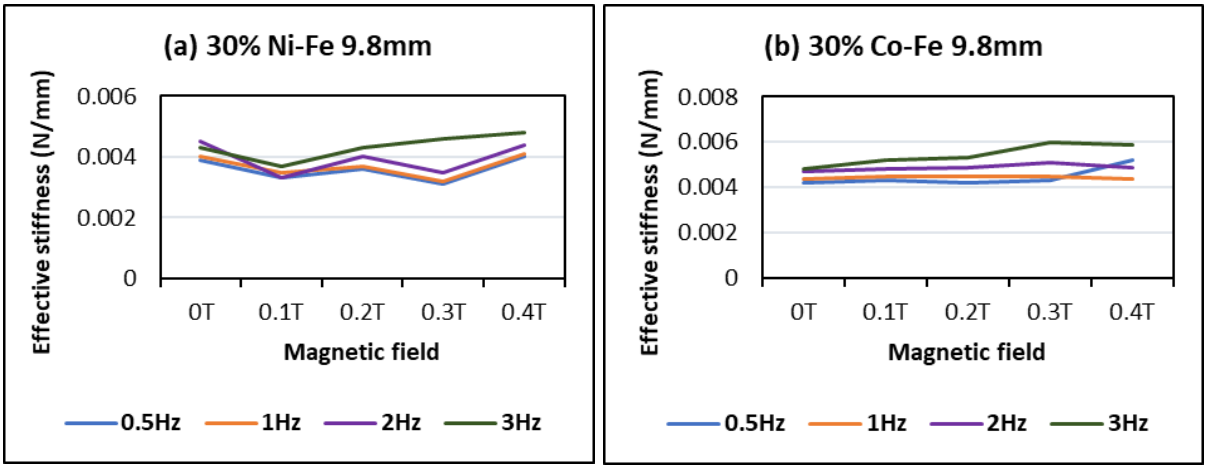

Figure 4.8 Effect of magnetic field and frequency on effective stiffness of (a) 30% Ni-Fe MRE and (b) 30% Co-Fe MRE

Figure 4.9 represents an evaluation of effective stiffness concerning magnetic field and strain amplitude. The graphs show increasing stiffness for increasing values of magnetic field. As discussed above the decrease in stiffness with increase in displacement amplitude can also be seen. The comparison of Co-Fe and Ni-Fe MREs shows higher stiffness values for Co-Fe MREs.

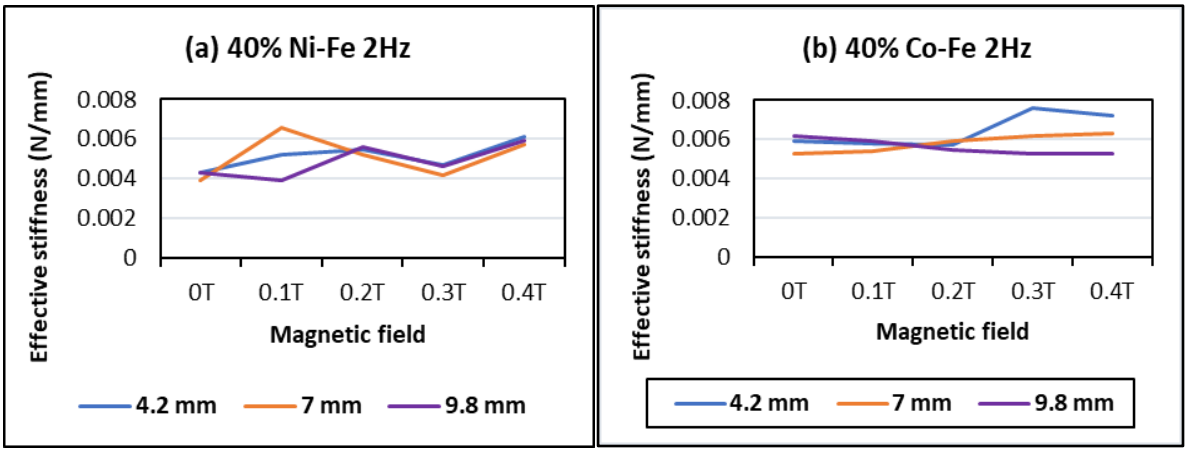

Figure 4.9 Effect of flux and displacement amplitude on effective stiffness of (a) 40% Ni-Fe MRE compared with (b) 40% Co-Fe MRE.

The MR effect refers to an MRE's sensitivity to an applied magnetic field [32]. The MR effect (%) here indicates the relative MR effect, which is calculated as the percentage increase in effective stiffness from 0 to 0.4 Tesla using equation (4.1***)***. *Figure 4.10* illustrates that the MR effect increases with the percentage of filler particles. This is due to the obvious reason that having a greater percentage of filler particles minimizes the gaps between them, which promotes particle interaction and results in a better response to a magnetic field. The gradual increase with % filler content can be seen in *Figure 4.10* (a) and it's true for all Ni-Fe samples at all frequencies and amplitudes except 30% Ni-Fe. The *Figure 4.10* (b) shows a representative MR effect trend for Co-Fe MREs, and this trend of decreasing MR effect for cobalt-iron samples, at high % content and high amplitude is consistent for all frequencies. The MR effect is shown to decrease with the large strains, i.e., the MR effect at 9.8 mm is always less than 4.2 mm. The literature explains this deterioration of the MR effect because of the increased spacing between the particles at large shear strains [54].

$$MR\ effect\ (\%) = \frac{keff\ (0.4T) - keff(0T)}{keff(0T)} \times 100 \qquad \textbf{(4.1)}$$

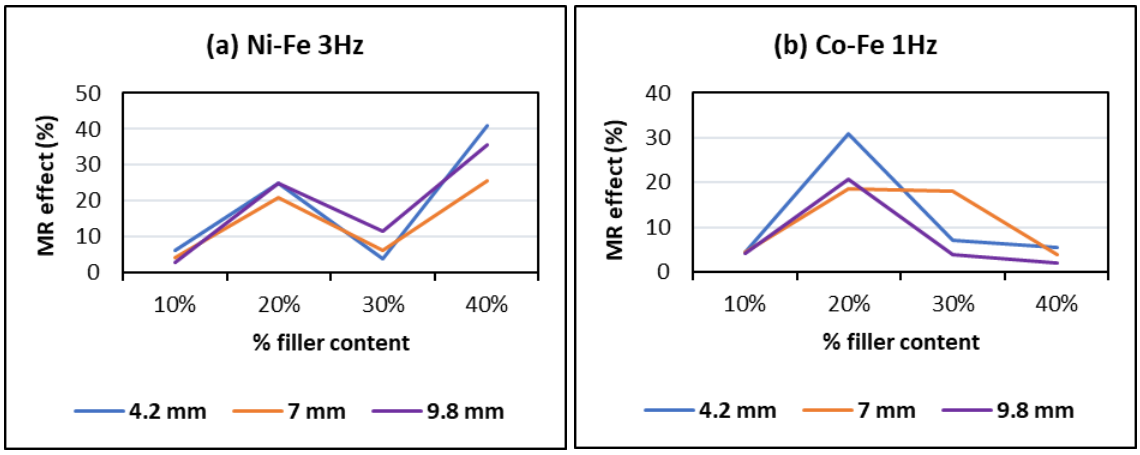

Figure 4.10 MR effect against every percentage of filler content for (a) Ni-Fe MREs and (b) Co-Fe MREs.

Figure 4.11 (a) shows the max MR effect values of all 8 samples. The maximum value of MR effect i.e., 55.56 at 1Hz frequency and 7 mm displacement amplitude for 40% Ni-Fe. The MR effect for Ni-Fe samples can be seen increasing with the filler content. The Co-Fe MRE showed maximum MR effect of 30.76% at 20% filler content, 1Hz frequency and 4.2mm displacement amplitude. The max MR effect for Co-Fe MRE is more than what was achieved with using only cobalt as a polarizable filler [45]. Although for Co-Fe samples increasing the % filler content decreases MR effect after a certain percentage. So, the optimum percentage for Co-Fe is between 20 and 30%. Figure 4.11 (b) shows max stiffness values representing Co-Fe having higher stiffness values as compared to Ni-Fe and maxi-mum stiffness of 0.0107 N/mm.

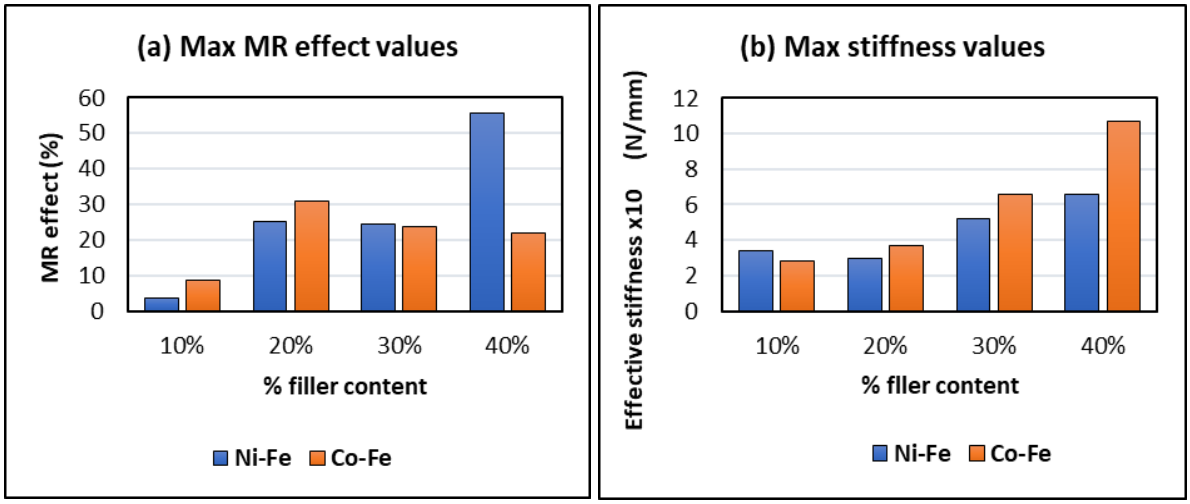

Figure 4.11 Comparison of (a) Maximum MR effect and (b) Maximum stiffness values for different %filler contents.

CONCLUSIONS

This article studied the effect of displacement amplitude, frequency, and magnetic field on the dynamic behavior of proposed hybrid MREs. The two kinds of MREs fabricated for this study incorporated nickel and cobalt particles along with iron particles as magnetically polarizable fillers. After the careful examination of the results from experimental testing the following conclusions can be obtained:

- The. MREs with Co-Fe as filler material have larger Payne effect i.e., the incremental decrease in effective stiffness of cobalt and iron filled MREs is more than nickel and iron MREs. This trend of strain-softening is intensified in the case of higher frequencies and larger magnetic fields.
- The strain rate stiffening effect for both Ni-Fe and Co-Fe was observed to be larger at small strains. For applied magnetic field the incremental stiffness increase for Ni-Fe was more than Co-Fe MREs.
- The highest MR effect obtained was 55.56% for nickel and iron filled MRE and 30.76% for Co-Fe MRE. The MREs with nickel and iron particles showed a trend of increasing MR effect with increasing % filler content; while for Co-Fe MRE the MR effect increased up to an optimum % and then decreased.
- The MREs with Cobalt and Iron particles gave higher stiffness while the MREs with Nickel and Iron gave higher MR effect.

FURTURE RESEARCH RECOMMENDATIONS

- This research shows that nickel particles when used with iron particles can give promising results in terms of both stiffness and MR effect. There were very less studies on nickel particles because of their less magnetic permeability. But now there could be further research carried out exploring the use of nickel particles in magneto-rheological elastomers.
- Cobalt particles can further be studied for optimum percentages in the elastomeric mix and for better MR effect.
- Nanoparticles of cobalt and nickel can be researched for their use in MR elastomers.
- Additives for MR elastomers can be explored for desired performance.

REFERENCES

[1] A.A. Markou, G. Stefanou, G.D. Manolis, Stochastic response of structures with hybrid base isolation systems, Eng. Struct. 172 (2018) 629–643. https://doi.org/10.1016/j.engstruct.2018.06.051.

[2] K. Miyamoto, D. Sato, J. She, A new performance index of LQR for combination of passive base isolation and active structural control, Eng. Struct. 157 (2018) 280–299. https://doi.org/10.1016/j.engstruct.2017.11.070.

[3] Y. Pei, Y. Liu, L. Zuo, Multi-resonant electromagnetic shunt in base isolation for vibration damping and energy harvesting, J. Sound Vib. 423 (2018) 1–17. https://doi.org/10.1016/j.jsv.2018.02.041.

[4] C. Ho, Y. Zhu, Z.Q. Lang, S.A. Billings, M. Kohiyama, S. Wakayama, Nonlinear damping based semi-active building isolation system, J. Sound Vib. 424 (2018) 302–317. https://doi.org/10.1016/j.jsv.2018.03.023.

[5] V. Lupășteanu, L. Soveja, R. Lupășteanu, C. Chingălată, Installation of a base isolation system made of friction pendulum sliding isolators in a historic masonry orthodox church, Eng. Struct. 188 (2019) 369–381. https://doi.org/10.1016/j.engstruct.2019.03.040.

[6] S. Cesmeci, F. Gordaninejad, K.L. Ryan, W. Eltahawy, Design of a fail-safe magnetorheological-based system for three-dimensional earthquake isolation of structures, Mechatronics. 64 (2019) 102296. https://doi.org/10.1016/j.mechatronics.2019.102296.

[7] D. Cancellara, F. De Angelis, Assessment and dynamic nonlinear analysis of different base isolation systems for a multi-storey RC building irregular in plan, Comput. Struct. 180 (2017) 74–88. https://doi.org/10.1016/j.compstruc.2016.02.012.

[8] H. Anajafi, R.A. Medina, Comparison of the seismic performance of a partial mass

isolation technique with conventional TMD and base-isolation systems under broad-band and narrow-band excitations, Eng. Struct. 158 (2018) 110–123. https://doi.org/10.1016/j.engstruct.2017.12.018.

[9] J. Pérez-Aracil, E. Pereira, I.M. Díaz, P. Reynolds, Passive and active vibration isolation under isolator-structure interaction: application to vertical excitations, Meccanica. 56 (2021) 1921–1935. https://doi.org/10.1007/s11012-021-01342-2.

[10] D. Leng, W. Feng, D. Ning, G. Liu, Analysis and design of a semi-active X-structured vibration isolator with magnetorheological elastomers, Mech. Syst. Signal Process. 181 (2022) 109492. https://doi.org/https://doi.org/10.1016/j.ymssp.2022.109492.

[11] A.K. Bastola, M. Hossain, A review on magneto-mechanical characterizations of magnetorheological elastomers, Compos. Part B Eng. 200 (2020) 108348. https://doi.org/10.1016/j.compositesb.2020.108348.

[12] D. Ivaneyko, V. Toshchevikov, M. Saphiannikova, G. Heinrich, Effects of particle distribution on mechanical properties of magneto-sensitive elastomers in a homogeneous magnetic field, Condens. Matter Phys. 15 (2012) 1–12. https://doi.org/10.5488/CMP.15.33601.

[13] P.R. von Lockette, J. Kadlowec, J.-H. Koo, Particle mixtures in magnetorheological elastomers (MREs), Smart Struct. Mater. 2006 Act. Mater. Behav. Mech. 6170 (2006) 61700T. https://doi.org/10.1117/12.658750.

[14] Y. Li, J. Li, Overview of the development of smart base isolation system featuring magnetorheological elastomer, Smart Struct. Syst. 24 (2019) 37–52. https://doi.org/10.12989/sss.2019.24.1.037.

[15] Y. Li, J. Li, On rate-dependent mechanical model for adaptive magnetorheological

elastomer base isolator, Smart Mater. Struct. 26 (2017) 45001. https://doi.org/10.1088/1361-665X/aa5f95.

[16] T.H. Nam, I. Petríková, B. Marvalová, Experimental characterization and viscoelastic modeling of isotropic and anisotropic magnetorheological elastomers, Polym. Test. 81 (2020). https://doi.org/10.1016/j.polymertesting.2019.106272.

[17] V. Kumar, D.J. Lee, Iron particle and anisotropic effects on mechanical properties of magneto-sensitive elastomers, J. Magn. Magn. Mater. 441 (2017) 105–112. https://doi.org/10.1016/j.jmmm.2017.05.049.

[18] M. Najib Alam, V. Kumar, S.R. Ryu, J. Choi, D.J. Lee, Magnetic response properties of natural-rubber-based magnetorhelogical elastomers with different-structured iron fillers, J. Magn. Magn. Mater. 513 (2020) 167106. https://doi.org/10.1016/j.jmmm.2020.167106.

[19] J. Winger, M. Schümann, A. Kupka, S. Odenbach, Influence of the particle size on the magnetorheological effect of magnetorheological elastomers, J. Magn. Magn. Mater. 481 (2019) 176–182. https://doi.org/10.1016/j.jmmm.2019.03.027.

[20] R.Z. Abd Rashid, N. Johari, S.A. Mazlan, S.A. Abdul Aziz, N.A. Nordin, N. Nazmi, S.N. Aqida, M.A.F. Johari, Effects of silica on mechanical and rheological properties of EPDM-based magnetorheological elastomers, Smart Mater. Struct. 30 (2021). https://doi.org/10.1088/1361-665X/ac1f64.

[21] J.-H. Koo, D.-D. Jang, M. Usman, H.-J. Jung, A feasibility study on smart base isolation systems using magneto-rheological elastomers, Struct. Eng. Mech. 32 (2009). https://doi.org/10.12989/sem.2009.32.6.755.

[22] A. Dargahi, R. Sedaghati, S. Rakheja, On the properties of magnetorheological elastomers in shear mode: Design, fabrication and characterization, Compos. Part B Eng. 159 (2019)

269–283. https://doi.org/10.1016/j.compositesb.2018.09.080.

[23] M. Usman, D.-D. Jang, I. Kim, H.-J. Jung, J. Koo, Dynamic testing and modeling of magneto-rheological elastomers, Proc. ASME 2009 Conf. Smart Mater. Adapt. Struct. Intell. Syst. (2009) 1–6.

[24] A. Bellelli, A. Spaggiari, Magneto-mechanical characterization of magnetorheological elastomers, J. Intell. Mater. Syst. Struct. 30 (2019) 2534–2543. https://doi.org/10.1177/1045389X19828828.

[25] M.A. Moreno, J. Gonzalez-Rico, M.L. Lopez-Donaire, A. Arias, D. Garcia-Gonzalez, New experimental insights into magneto-mechanical rate dependences of magnetorheological elastomers, Compos. Part B Eng. 224 (2021) 109148. https://doi.org/10.1016/j.compositesb.2021.109148.

[26] I.A. Perales-Martínez, L.M. Palacios-Pineda, L.M. Lozano-Sánchez, O. Martínez-Romero, J.G. Puente-Cordova, A. Elías-Zúñiga, Enhancement of a magnetorheological PDMS elastomer with carbonyl iron particles, Polym. Test. 57 (2017) 78–86. https://doi.org/10.1016/j.polymertesting.2016.10.029.

[27] M. Asadi Khanouki, R. Sedaghati, M. Hemmatian, Experimental characterization and microscale modeling of isotropic and anisotropic magnetorheological elastomers, Compos. Part B Eng. 176 (2019) 107311. https://doi.org/10.1016/j.compositesb.2019.107311.

[28] M.N. Alam, V. Kumar, D.J. Lee, J. Choi, Magnetically active response of acrylonitrile-butadiene-rubber-based magnetorheological elastomers with different types of iron fillers and their hybrid, Compos. Commun. 24 (2021) 100657. https://doi.org/10.1016/j.coco.2021.100657.

[29] L. Cestarollo, S. Smolenski, A. El-Ghazaly, Nanoparticle-Based Magnetorheological Elastomers with Enhanced Mechanical Deflection for Haptic Displays, ACS Appl. Mater. Interfaces. 14 (2022) 19002–19011. https://doi.org/10.1021/acsami.2c05471.

[30] S.U. Khayam, M. Usman, M.A. Umer, A. Rafique, Development and characterization of a novel hybrid magnetorheological elastomer incorporating micro and nano size iron fillers, Mater. Des. 192 (2020). https://doi.org/10.1016/j.matdes.2020.108748.

[31] D. Gorman, N. Murphy, R. Ekins, S. Jerrams, The evaluation of the effect of strain limits on the physical properties of Magnetorheological Elastomers subjected to uniaxial and biaxial cyclic testing, Int. J. Fatigue. 103 (2017) 1–4. https://doi.org/10.1016/j.ijfatigue.2017.05.011.

[32] H. Vatandoost, S. Rakheja, R. Sedaghati, Effects of iron particles' volume fraction on compression mode properties of magnetorheological elastomers, J. Magn. Magn. Mater. 522 (2021). https://doi.org/10.1016/j.jmmm.2020.167552.

[33] M.A. Hafeez, M. Usman, M.A. Umer, A. Hanif, Recent progress in isotropic magnetorheological elastomers and their properties: A review, Polymers (Basel). 12 (2020) 1–35. https://doi.org/10.3390/polym12123023.

[34] V. Kumar, J.Y. Lee, D.J. Lee, The response force and rate of magneto-rheological elastomers with different fillers and magnetic fields, J. Magn. Magn. Mater. 466 (2018) 164–171. https://doi.org/10.1016/j.jmmm.2018.06.072.

[35] M. Usman, H. Jung, Recent developments of magneto- rheological elastomers for civil engineering applications, in: Smart Mater. Actuators Recent Adv. Charact. Appl., 2015.

[36] S.A.A. Aziz, S.A. Mazlan, U. Ubaidillah, M.K. Shabdin, N.A. Yunus, N.A. Nordin, S.B. Choi, R.M. Rosnan, Enhancement of viscoelastic and electrical properties of

magnetorheological elastomers with nanosized Ni-Mg cobalt-ferrites as fillers, Materials (Basel). 12 (2019) 1–18. https://doi.org/10.3390/ma12213531.

[37] E.Y. Kramarenko, A. V. Chertovich, G. V. Stepanov, A.S. Semisalova, L.A. Makarova, N.S. Perov, A.R. Khokhlov, Magnetic and viscoelastic response of elastomers with hard magnetic filler, Smart Mater. Struct. 24 (2015) 35002. https://doi.org/10.1088/0964-1726/24/3/035002.

[38] J.Y. Lee, V. Kumar, D.J. Lee, Compressive properties of magnetorheological elastomer with different magnetic fields and types of filler, Polym. Adv. Technol. 30 (2019) 1106–1115. https://doi.org/10.1002/pat.4544.

[39] I. Bica, The influence of the magnetic field on the elastic properties of anisotropic magnetorheological elastomers, J. Ind. Eng. Chem. 18 (2012) 1666–1669. https://doi.org/10.1016/j.jiec.2012.03.006.

[40] H.J. Song, O. Padalka, N.M. Wereley, R.C. Bell, Impact of nanowire versus spherical microparticles in magnetorheological elastomer composites, Collect. Tech. Pap. - AIAA/ASME/ASCE/AHS/ASC Struct. Struct. Dyn. Mater. Conf. (2009) 1–10. https://doi.org/10.2514/6.2009-2118.

[41] J. Berasategi, D. Salazar, A. Gomez, J. Gutierrez, M.S. Sebastián, M. Bou-Ali, J.M. Barandiaran, Anisotropic behaviour analysis of silicone/carbonyl iron particles magnetorheological elastomers, Rheol. Acta. 59 (2020) 469–476. https://doi.org/10.1007/s00397-020-01218-4.

[42] Y. Tong, X. Dong, M. Qi, Improved tunable range of the field-induced storage modulus by using flower-like particles as the active phase of magnetorheological elastomers, Soft Matter. 14 (2018) 3504–3509. https://doi.org/10.1039/c8sm00359a.

[43] J.R. Davis, ASM Specialty Handbook: Nickel, Cobalt, and Their Alloys, ASM International, 2000.

[44] D.H. Huang, T.N. Tran, B. Yang, Investigation on the reaction of iron powder mixture as a portable heat source for thermoelectric power generators, J. Therm. Anal. Calorim. 116 (2014) 1047–1053. https://doi.org/10.1007/s10973-013-3619-9.

[45] A.A. Zainudin, N.A. Yunus, S.A. Mazlan, M.K. Shabdin, S.A. Aziz Abdul, N.A. Nordin, N. Nazmi, M.A.A. Rahman, Rheological and resistance properties of magnetorheological elastomer with cobalt for sensor application, Appl. Sci. 10 (2020). https://doi.org/10.3390/app10051638.

[46] O. Padalka, H.J. Song, N.M. Wereley, J.A. Filer, R.C. Bell, Stiffness and damping in Fe, Co, and Ni nanowire-based magnetorheological elastomeric composites, IEEE Trans. Magn. 46 (2010) 2275–2277. https://doi.org/10.1109/TMAG.2010.2044759.

[47] N. Moksin, H. Ismail, M.K. Abdullah, R.K. Shuib, Magnetorheological elastomer composites based on industrial waste nickel zinc ferrite and natural rubber, Rubber Chem. Technol. 92 (2019) 749–762. https://doi.org/10.5254/RCT.19.81505.

[48] H.J. Jung, S.J. Lee, D.D. Jang, I.H. Kim, J.H. Koo, F. Khan, Dynamic characterization of magneto-rheological elastomers in shear mode, IEEE Trans. Magn. 45 (2009) 3930–3933. https://doi.org/10.1109/TMAG.2009.2024886.

[49] G. Schubert, P. Harrison, Large-strain behaviour of Magneto-Rheological Elastomers tested under uniaxial compression and tension, and pure shear deformations, Polym. Test. 42 (2015) 122–134. https://doi.org/10.1016/j.polymertesting.2015.01.008.

[50] F. Gordaninejad, X. Wang, P. Mysore, Behavior of thick magnetorheological elastomers, J. Intell. Mater. Syst. Struct. 23 (2012) 1033–1039.

https://doi.org/10.1177/1045389X12448286.

[51] H. Vatandoost, M. Hemmatian, R. Sedaghati, S. Rakheja, Dynamic characterization of isotropic and anisotropic magnetorheological elastomers in the oscillatory squeeze mode superimposed on large static pre-strain, Compos. Part B Eng. 182 (2020). https://doi.org/10.1016/j.compositesb.2019.107648.

[52] I. Agirre-Olabide, M.J. Elejabarrieta, A new magneto-dynamic compression technique for magnetorheological elastomers at high frequencies, Polym. Test. 66 (2018) 114–121. https://doi.org/10.1016/j.polymertesting.2018.01.011.

[53] M. Norouzi, S.M. Sajjadi Alehashem, H. Vatandoost, Y.Q. Ni, M.M. Shahmardan, A new approach for modeling of magnetorheological elastomers, J. Intell. Mater. Syst. Struct. 27 (2016) 1121–1135. https://doi.org/10.1177/1045389X15615966.

[54] M.F. Jaafar, F. Mustapha, M. Mustapha, Review of current research progress related to magnetorheological elastomer material, J. Mater. Res. Technol. 15 (2021) 5010–5045. https://doi.org/https://doi.org/10.1016/j.jmrt.2021.10.058.

PUBLICATION

1. S. Tahir, M. Usman, M.A. Umer, Effect of Volume Fraction on Shear Mode Properties of Fe-Co and Fe-Ni Filled Magneto-Rheological Elastomers, Polymers (Basel). 14 (2022) 2968. https://doi.org/10.3390/polym14142968.

Appendix A: Supplementary Results

A1 Effect of amplitude

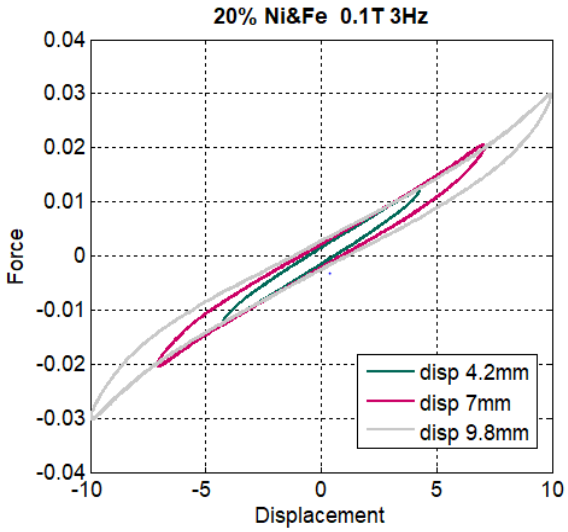

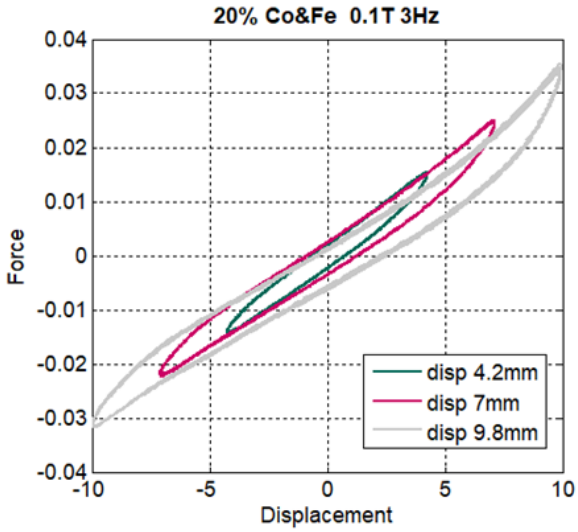

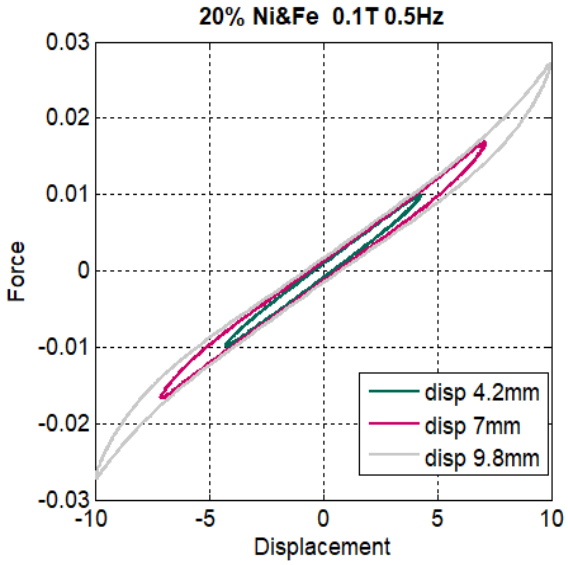

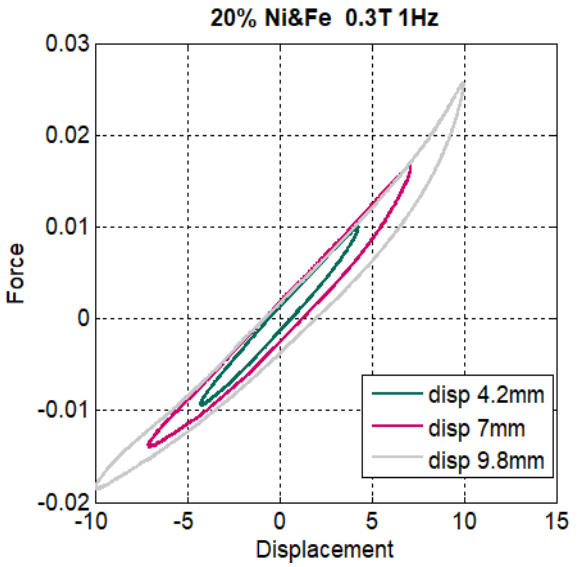

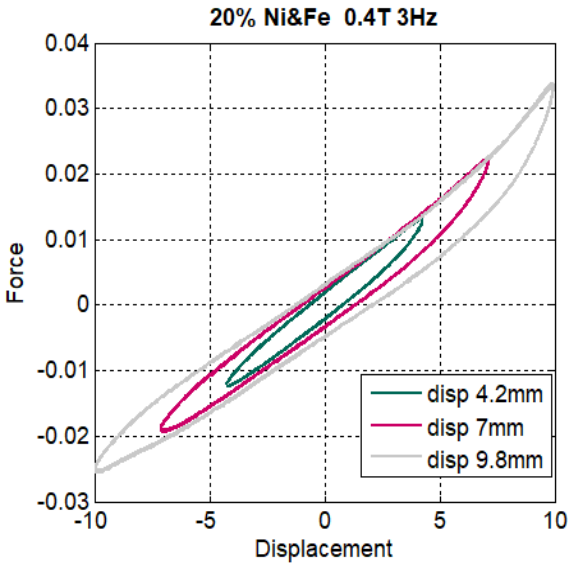
20% Ni&Fe 0.4T 3Hz
Force
Displacement
disp 4.2mm
disp 7mm
disp 9.8mm

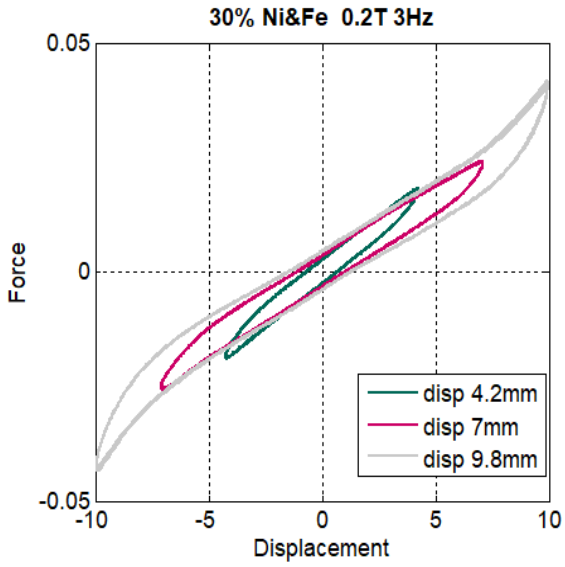
30% Ni&Fe 0.2T 3Hz
Force
Displacement
disp 4.2mm
disp 7mm
disp 9.8mm

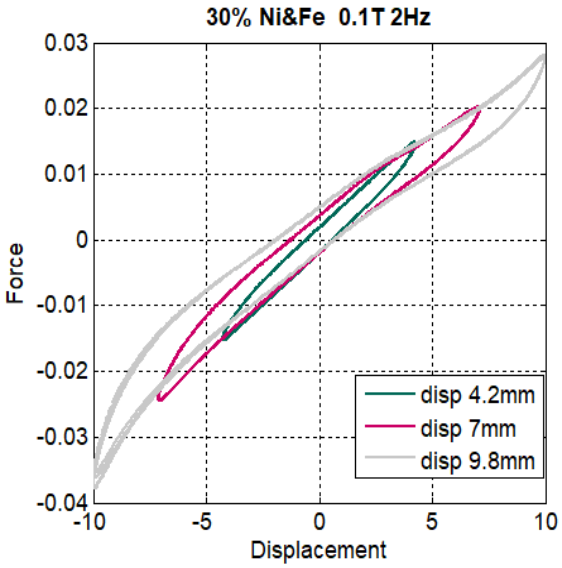
30% Ni&Fe 0.1T 2Hz
Force
Displacement
disp 4.2mm
disp 7mm
disp 9.8mm

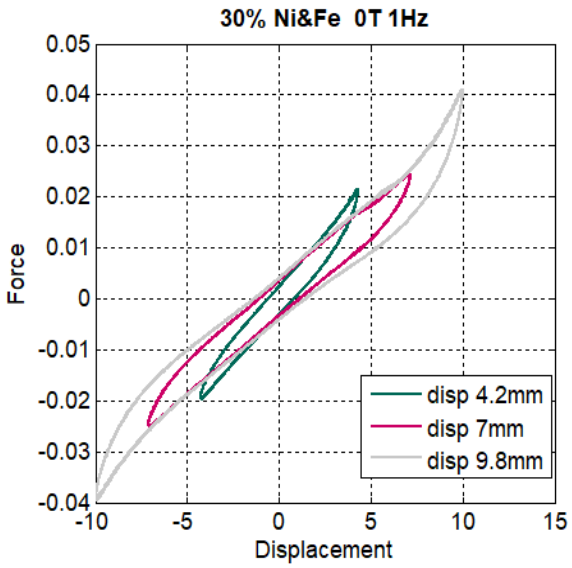
30% Ni&Fe 0T 1Hz
Force
Displacement
disp 4.2mm
disp 7mm
disp 9.8mm

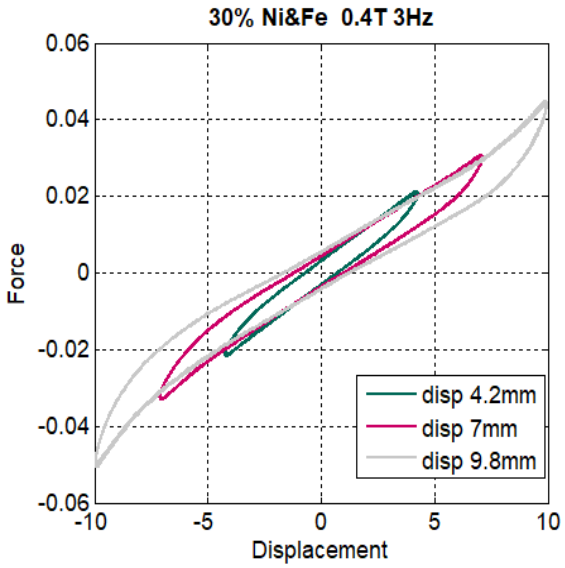
30% Ni&Fe 0.4T 3Hz
Force
Displacement
disp 4.2mm
disp 7mm
disp 9.8mm

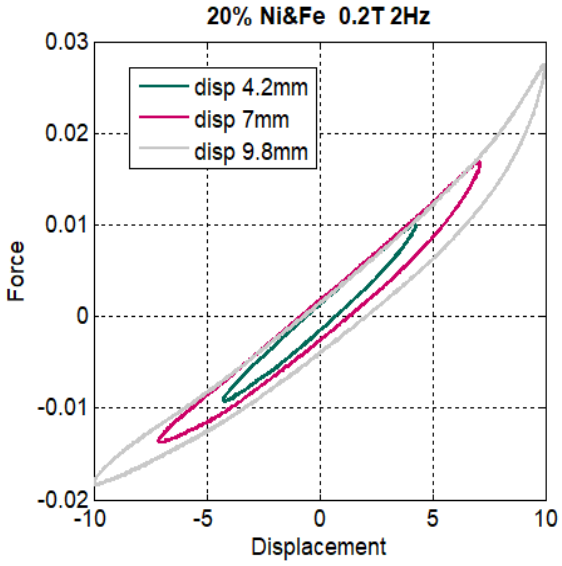
20% Ni&Fe 0.2T 2Hz
Force
Displacement
disp 4.2mm
disp 7mm
disp 9.8mm

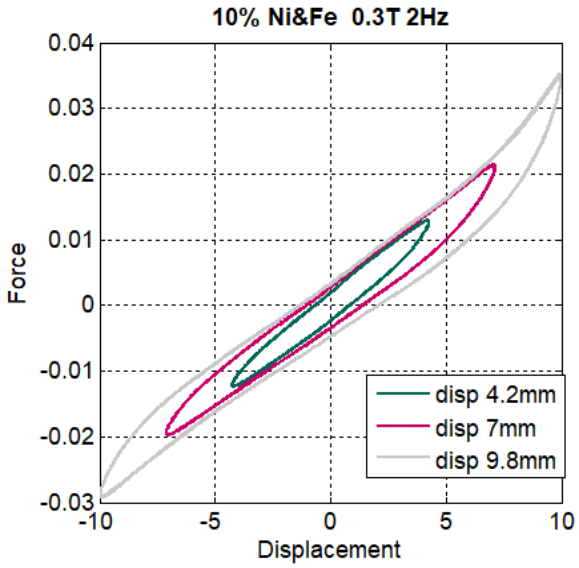
10% Ni&Fe 0.3T 2Hz
Force
Displacement
disp 4.2mm
disp 7mm
disp 9.8mm

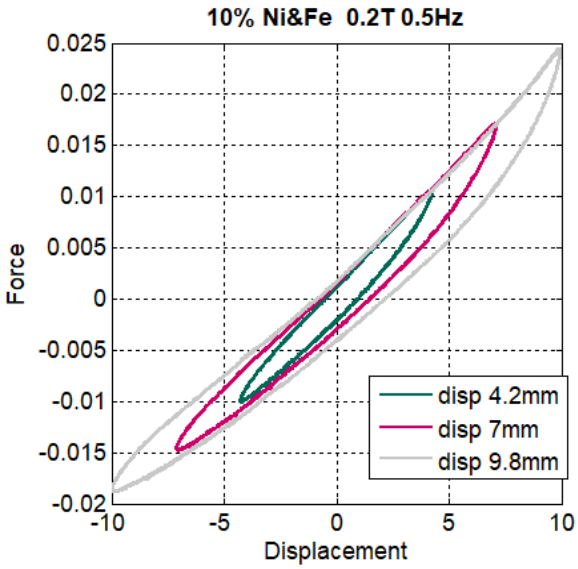
10% Ni&Fe 0.2T 0.5Hz
Force
Displacement
disp 4.2mm
disp 7mm
disp 9.8mm

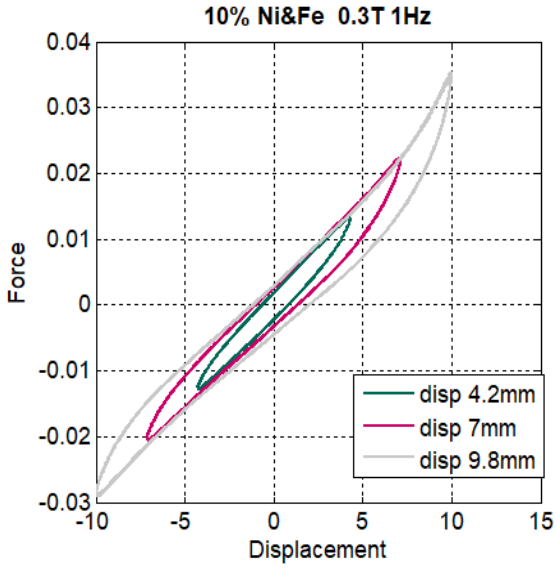
10% Ni&Fe 0.3T 1Hz
Force
Displacement
disp 4.2mm
disp 7mm
disp 9.8mm

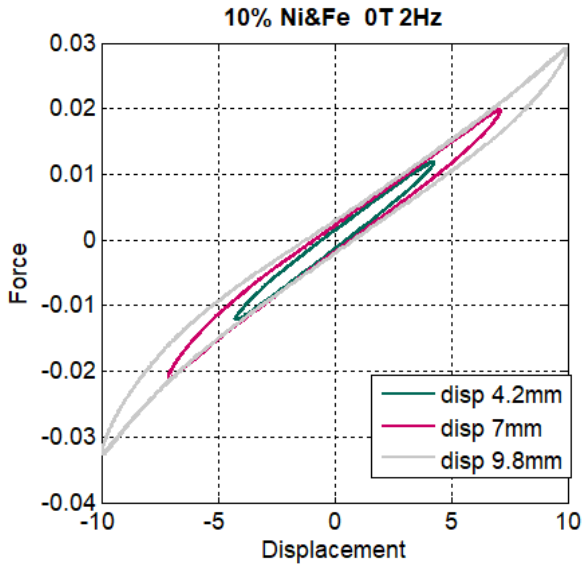
10% Ni&Fe 0T 2Hz
Force
Displacement
disp 4.2mm
disp 7mm
disp 9.8mm

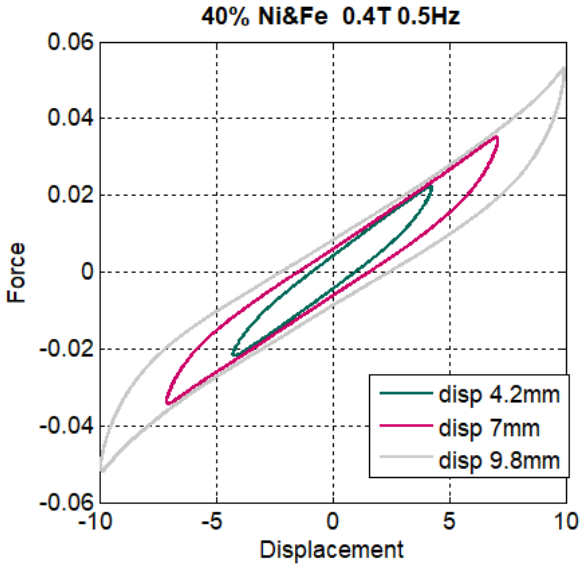
40% Ni&Fe 0.4T 0.5Hz
Force
Displacement
disp 4.2mm
disp 7mm
disp 9.8mm

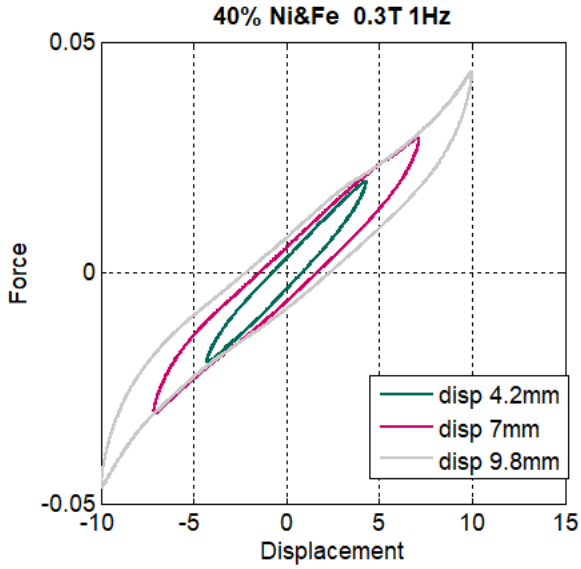
40% Ni&Fe 0.3T 1Hz
Force
Displacement
disp 4.2mm
disp 7mm
disp 9.8mm

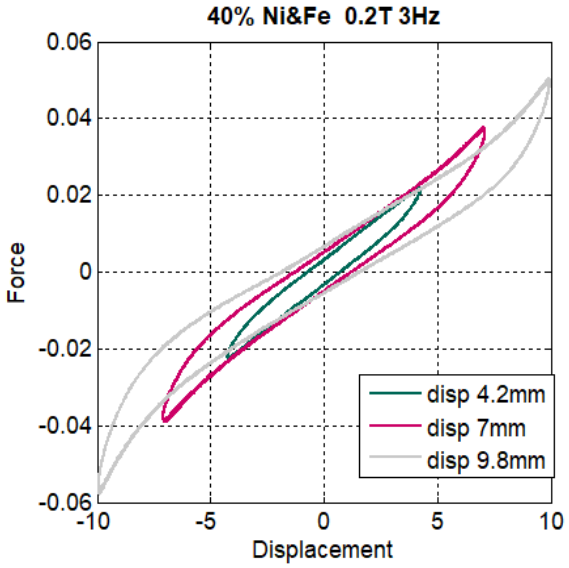
40% Ni&Fe 0.2T 3Hz
Force
Displacement
disp 4.2mm
disp 7mm
disp 9.8mm

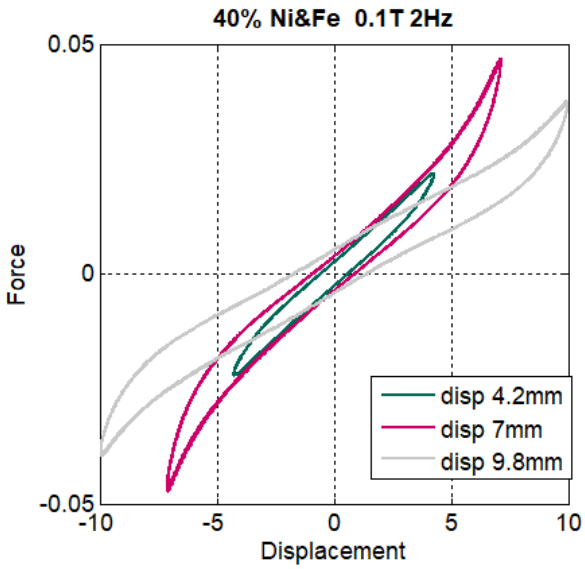
40% Ni&Fe 0.1T 2Hz
Force
Displacement
disp 4.2mm
disp 7mm
disp 9.8mm

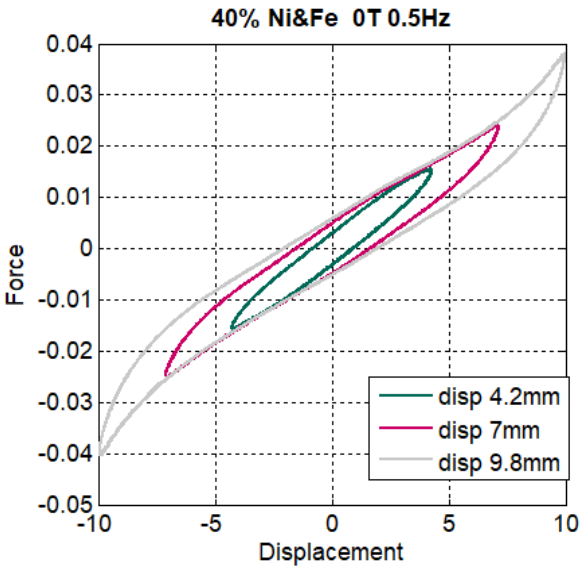
40% Ni&Fe 0T 0.5Hz
Force
Displacement
disp 4.2mm
disp 7mm
disp 9.8mm

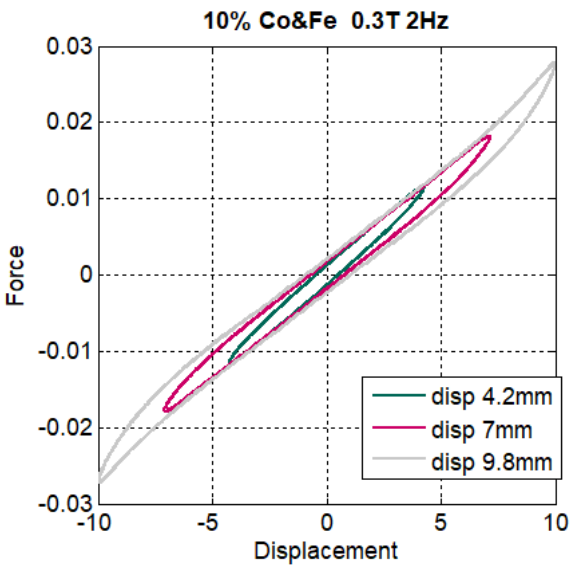
10% Co&Fe 0.3T 2Hz
Force
Displacement
disp 4.2mm
disp 7mm
disp 9.8mm

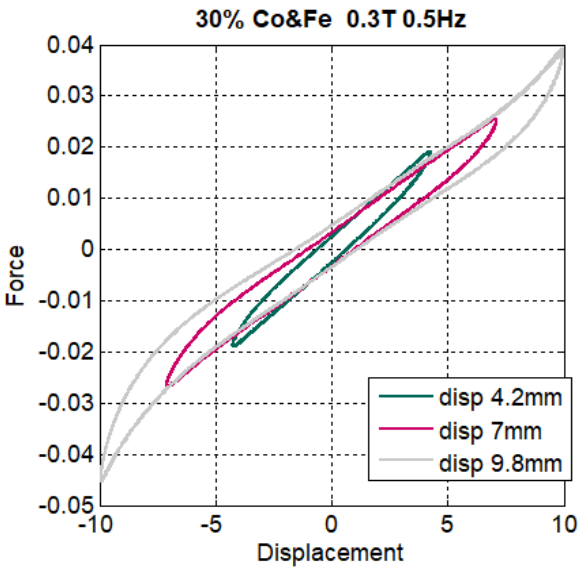
30% Co&Fe 0.3T 0.5Hz
Force
Displacement
disp 4.2mm
disp 7mm
disp 9.8mm

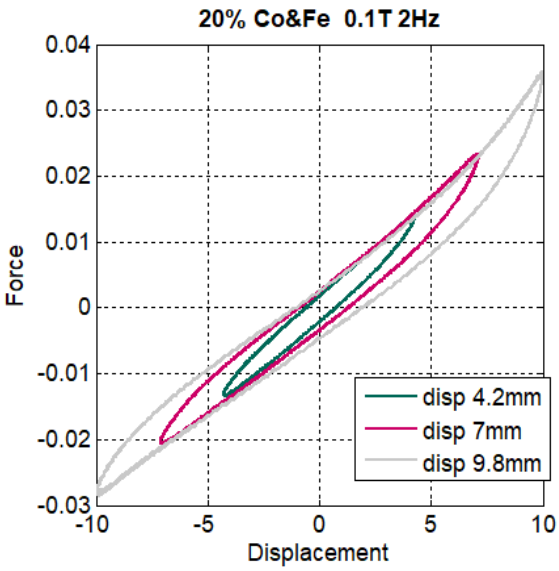
20% Co&Fe 0.1T 2Hz
Force
Displacement
disp 4.2mm
disp 7mm
disp 9.8mm

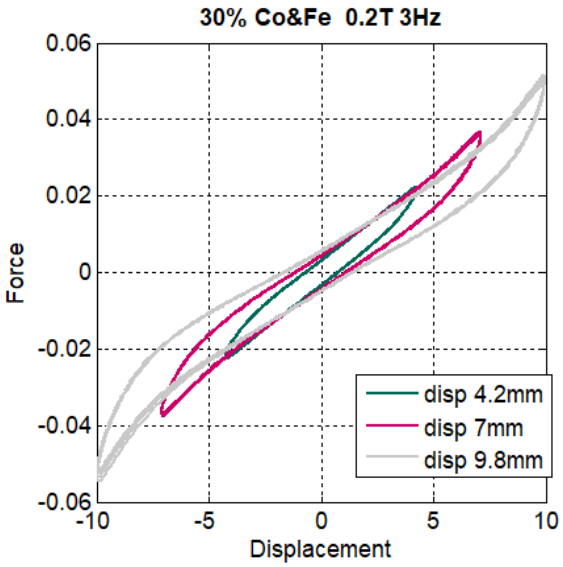
30% Co&Fe 0.2T 3Hz
Force
Displacement
disp 4.2mm
disp 7mm
disp 9.8mm

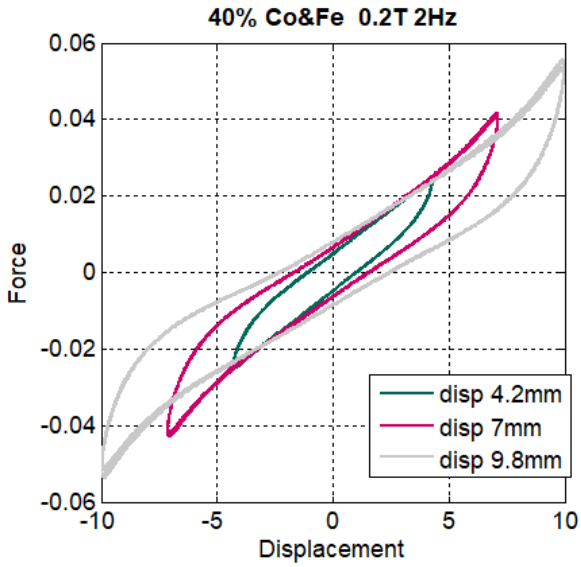
40% Co&Fe 0.2T 2Hz
Force
Displacement
disp 4.2mm
disp 7mm
disp 9.8mm

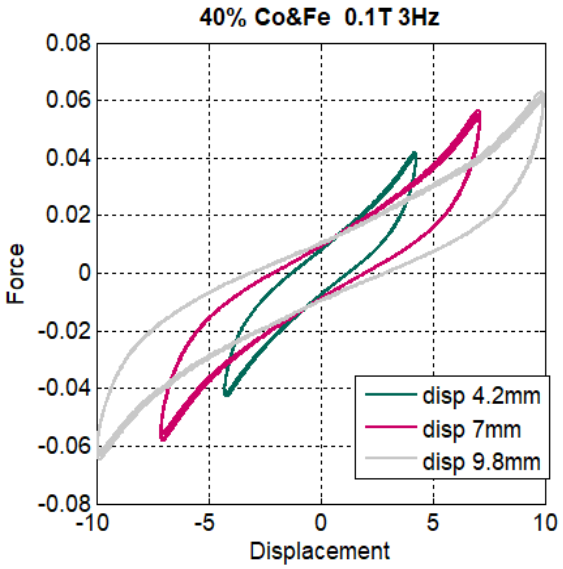
40% Co&Fe 0.1T 3Hz
Force
Displacement
disp 4.2mm
disp 7mm
disp 9.8mm

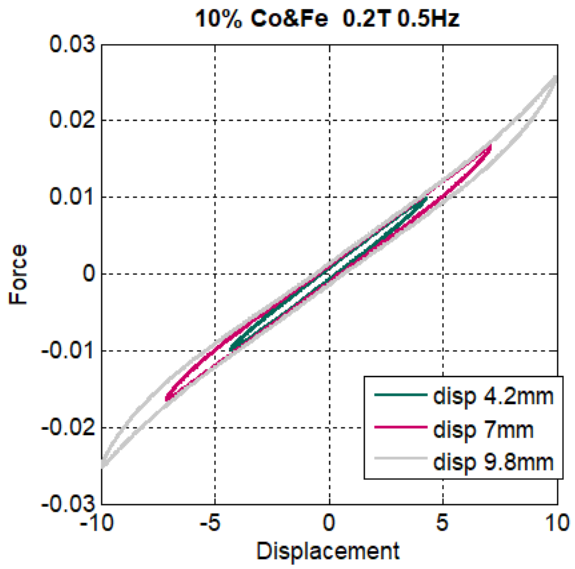
10% Co&Fe 0.2T 0.5Hz
Force
Displacement
disp 4.2mm
disp 7mm
disp 9.8mm

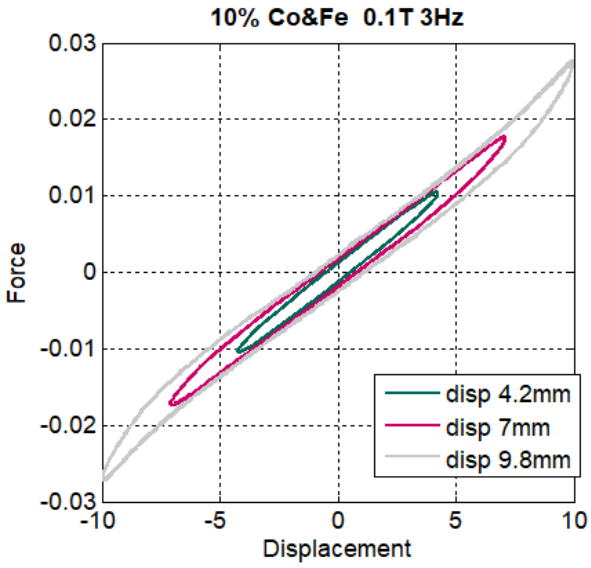
10% Co&Fe 0.1T 3Hz
Force
Displacement
disp 4.2mm
disp 7mm
disp 9.8mm

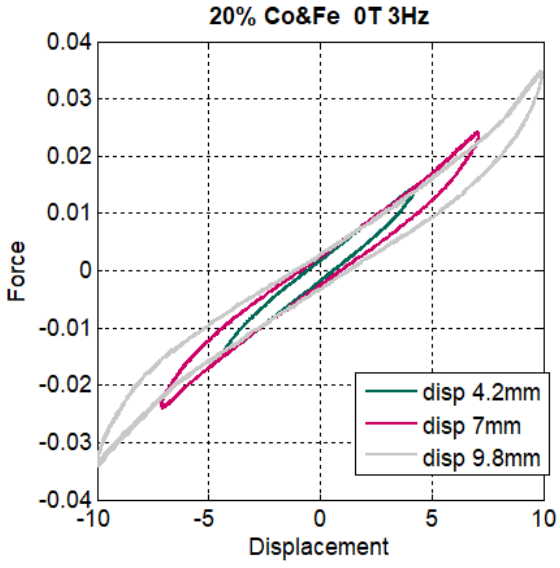
20% Co&Fe 0T 3Hz
Force
Displacement
disp 4.2mm
disp 7mm
disp 9.8mm

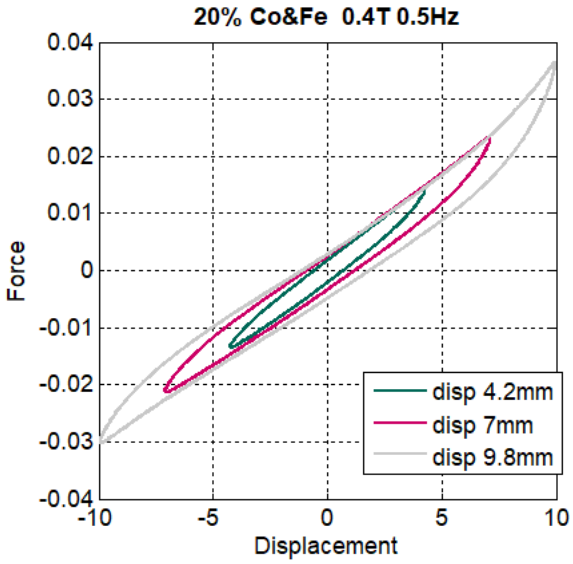

A2 Effect of frequency

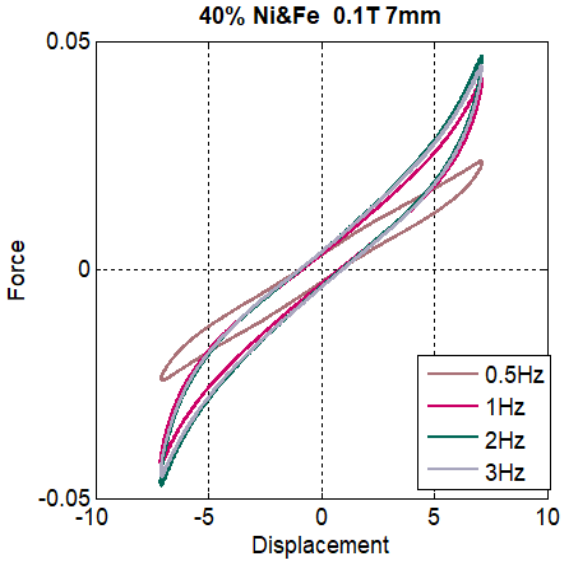

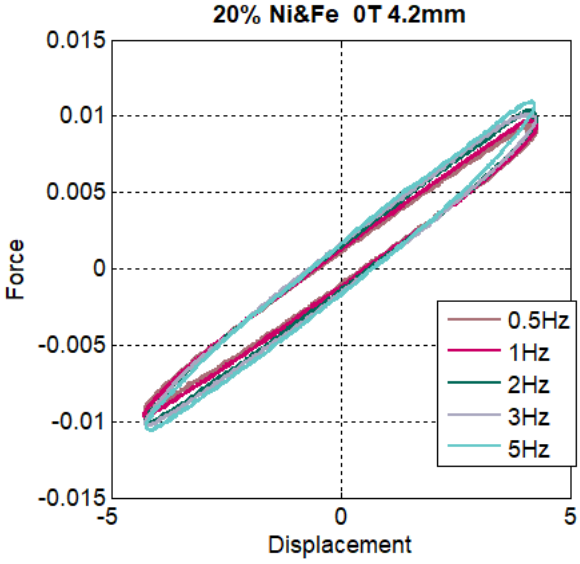

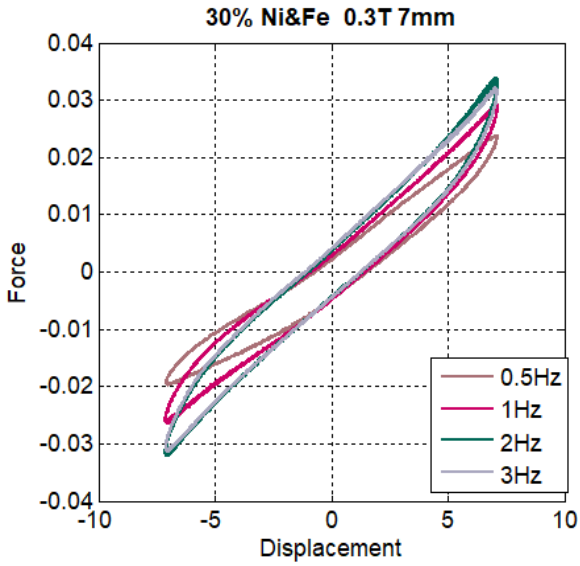
30% Ni&Fe 0.3T 7mm
Force
Displacement
0.5Hz
1Hz
2Hz
3Hz

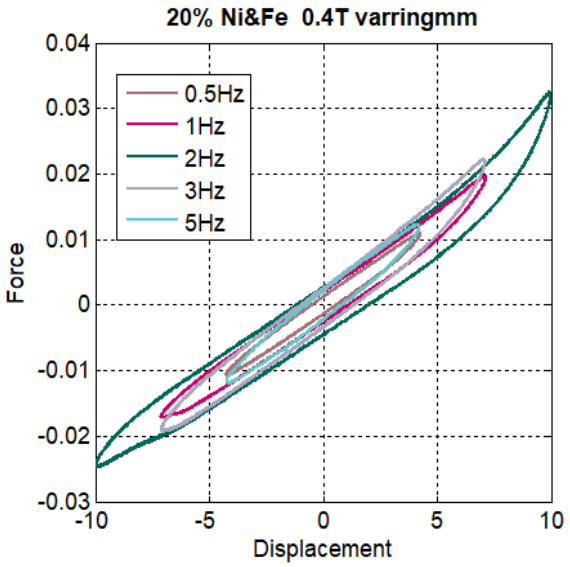
20% Ni&Fe 0.4T varringmm
Force
Displacement
0.5Hz
1Hz
2Hz
3Hz
5Hz

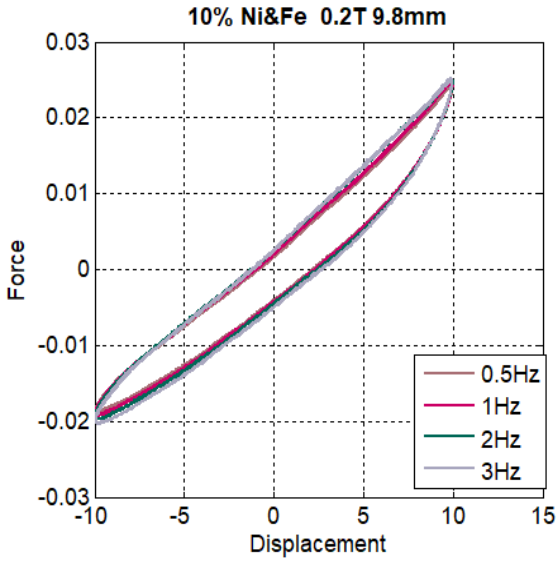
10% Ni&Fe 0.2T 9.8mm
Force
Displacement
0.5Hz
1Hz
2Hz
3Hz

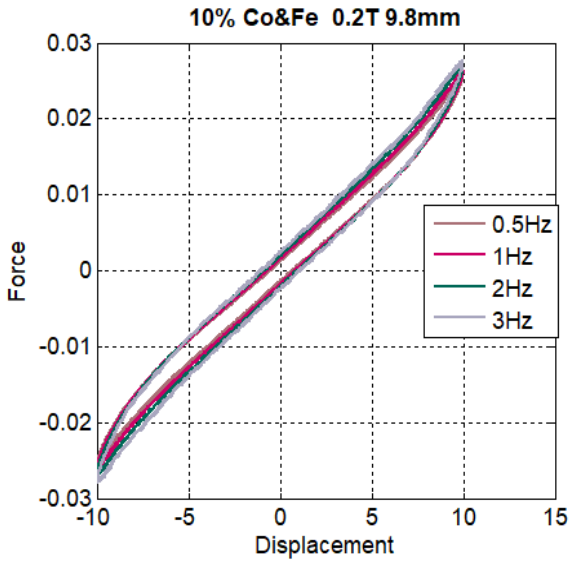
10% Co&Fe 0.2T 9.8mm
Force
Displacement
0.5Hz
1Hz
2Hz
3Hz

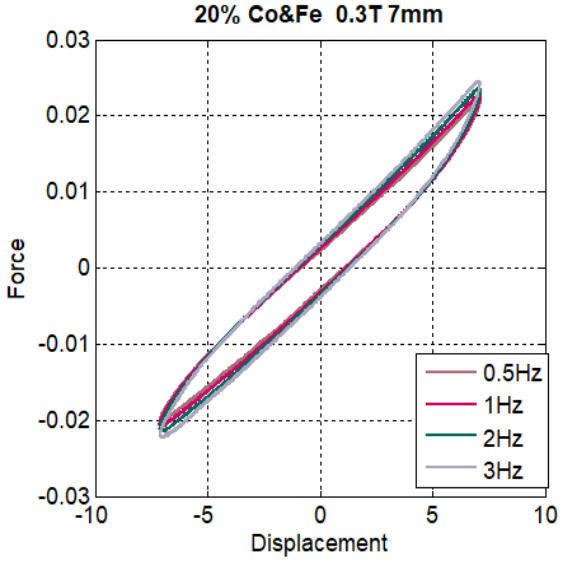
20% Co&Fe 0.3T 7mm
Force
Displacement
0.5Hz
1Hz
2Hz
3Hz

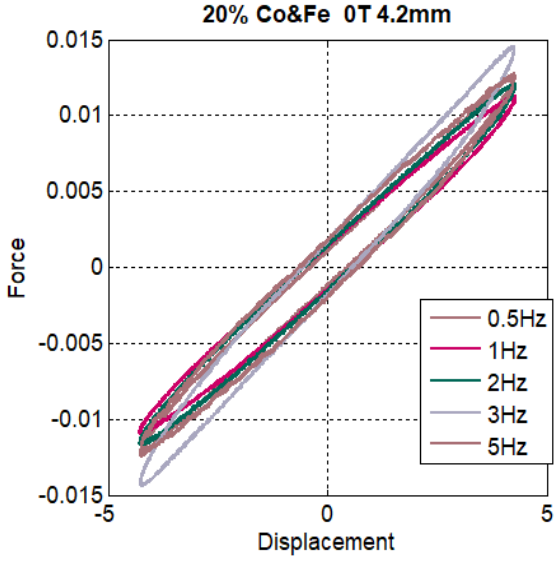
20% Co&Fe 0T 4.2mm
Force
Displacement
0.5Hz
1Hz
2Hz
3Hz
5Hz

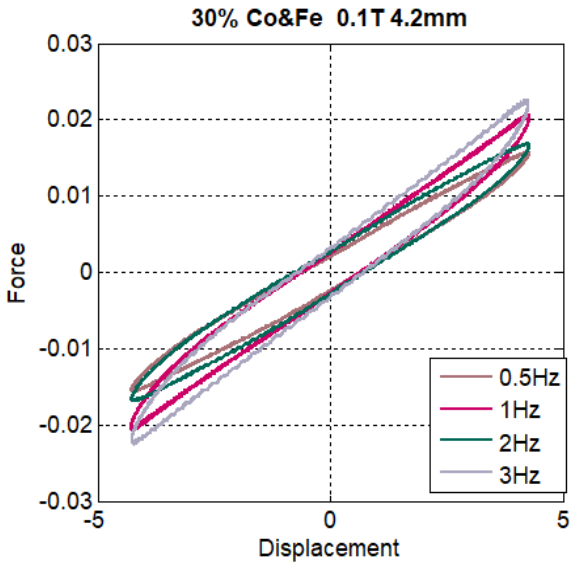
30% Co&Fe 0.1T 4.2mm
Force
Displacement
0.5Hz
1Hz
2Hz
3Hz

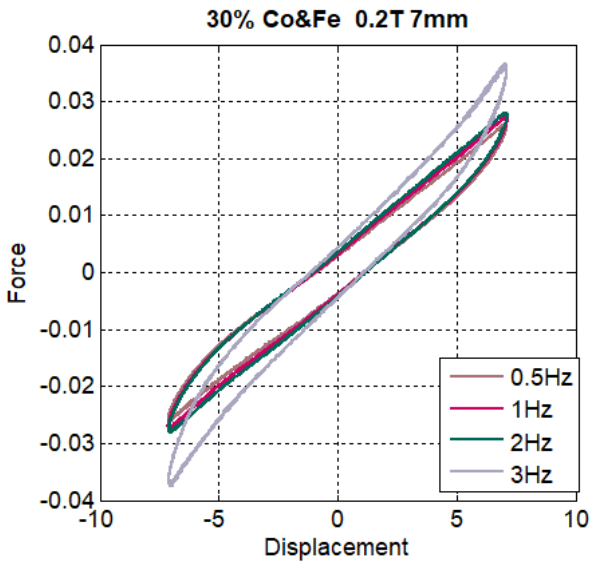
30% Co&Fe 0.2T 7mm
Force
Displacement
0.5Hz
1Hz
2Hz
3Hz

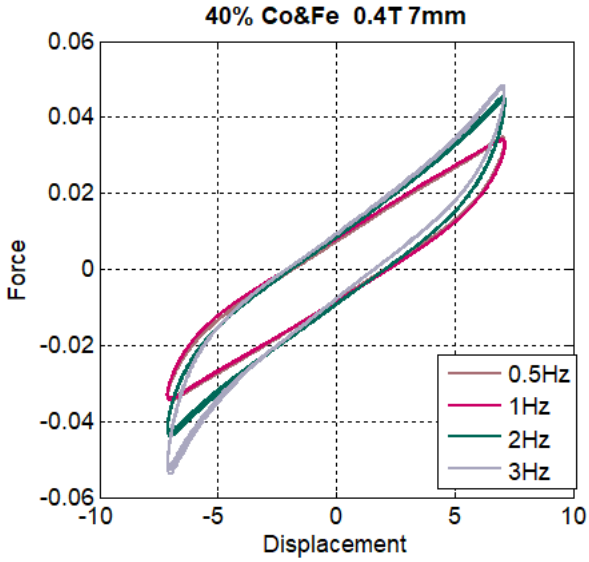
40% Co&Fe 0.4T 7mm
Force
Displacement
0.5Hz
1Hz
2Hz
3Hz

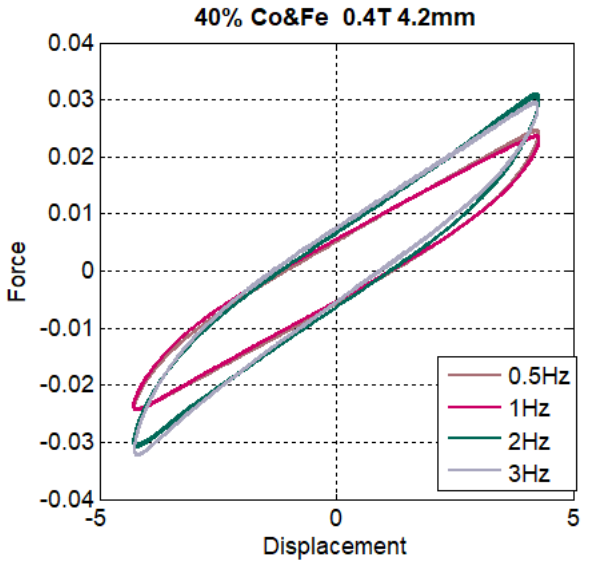
40% Co&Fe 0.4T 4.2mm
Force
Displacement
0.5Hz
1Hz
2Hz
3Hz

A3 Effect of magnetic field

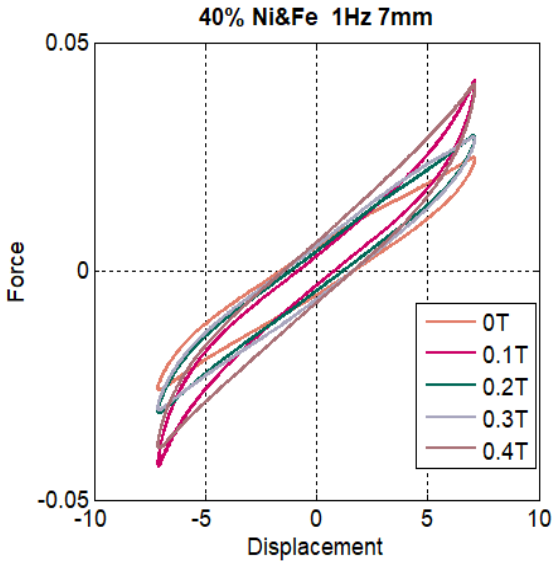

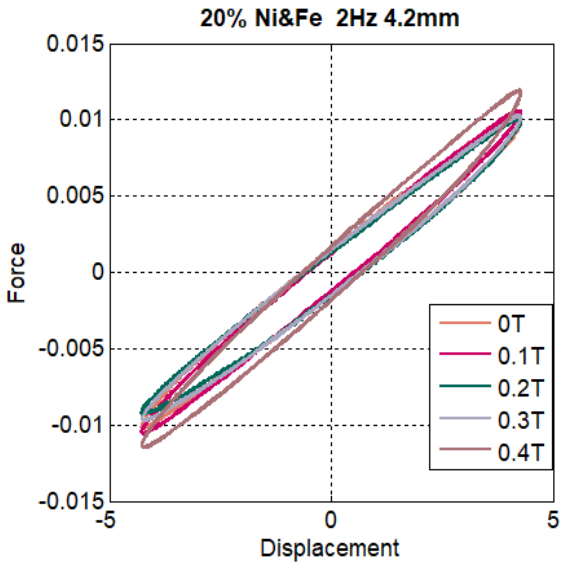

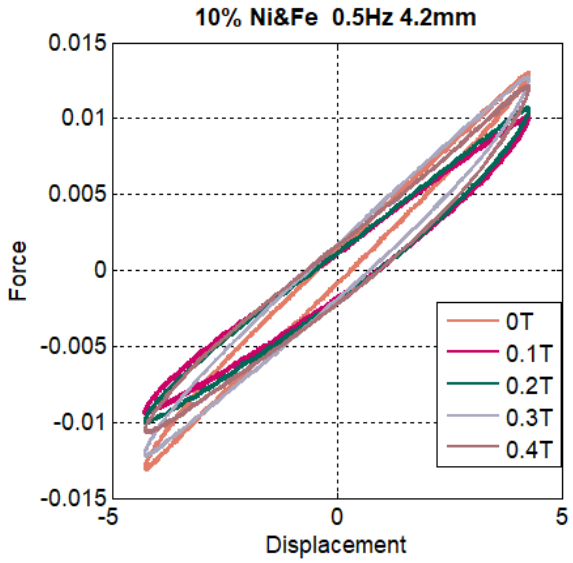

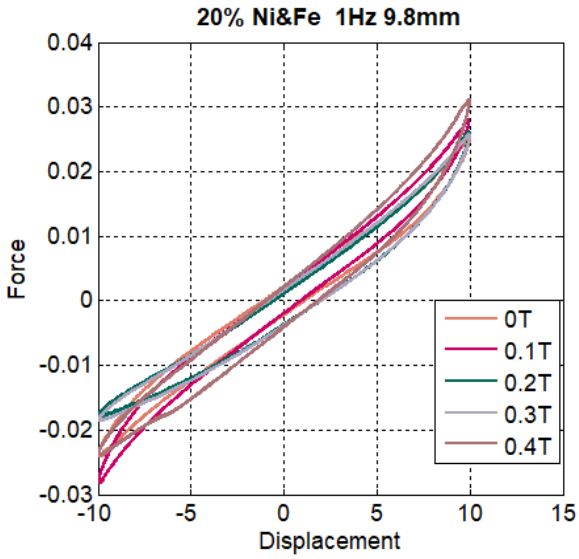

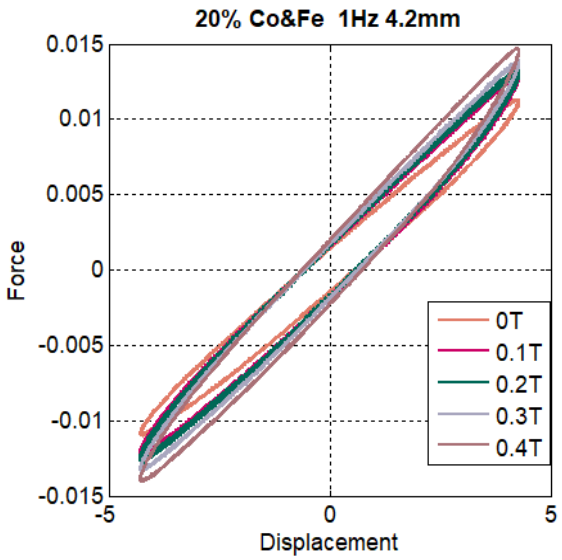
20% Co&Fe 1Hz 4.2mm
Force
Displacement
0T
0.1T
0.2T
0.3T
0.4T

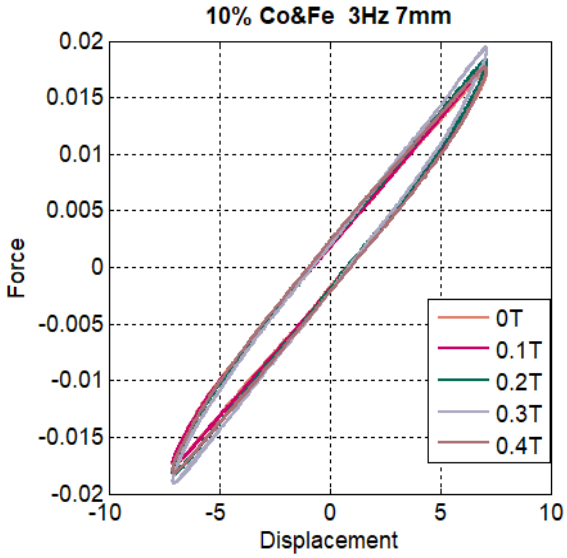
10% Co&Fe 3Hz 7mm
Force
Displacement
0T
0.1T
0.2T
0.3T
0.4T

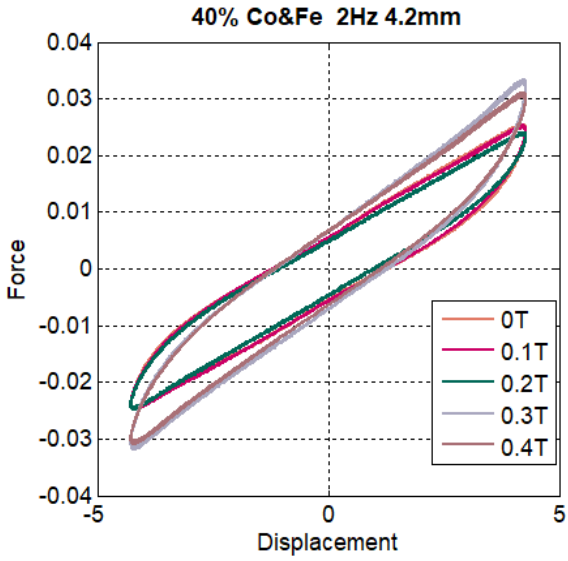
40% Co&Fe 2Hz 4.2mm
Force
Displacement
0T
0.1T
0.2T
0.3T
0.4T

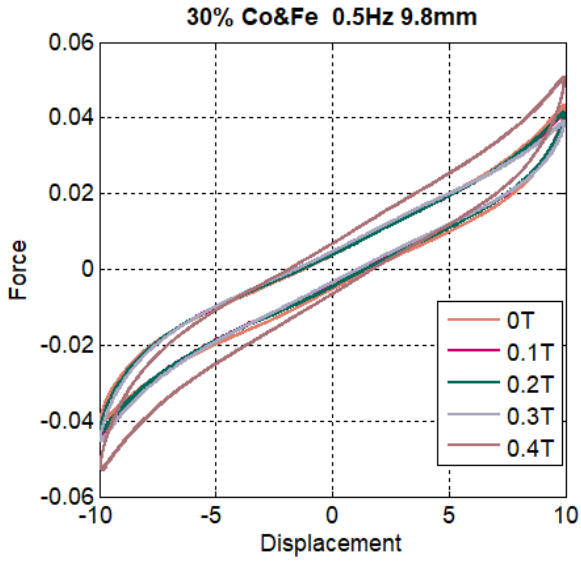
30% Co&Fe 0.5Hz 9.8mm
Force
Displacement
0T
0.1T
0.2T
0.3T
0.4T

A4 Other results

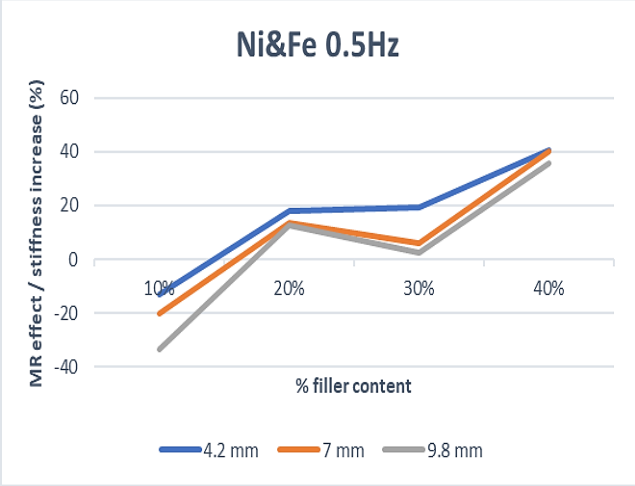

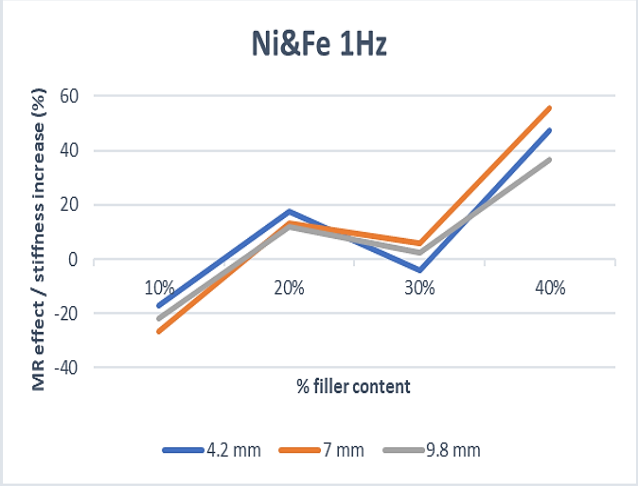

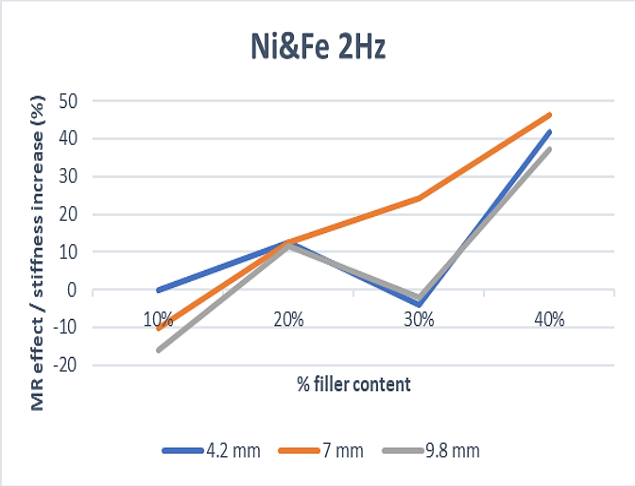

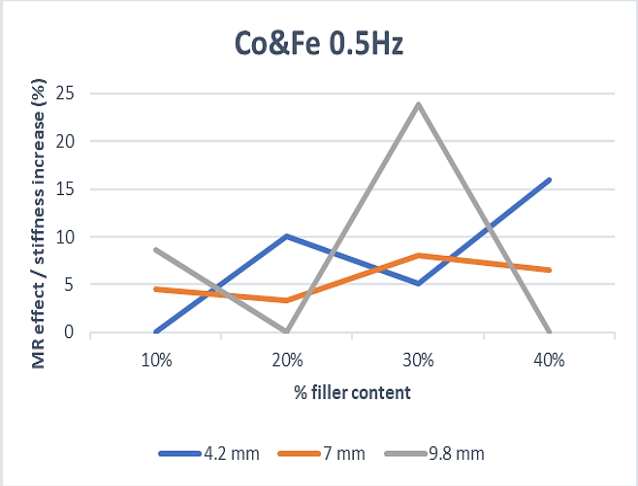

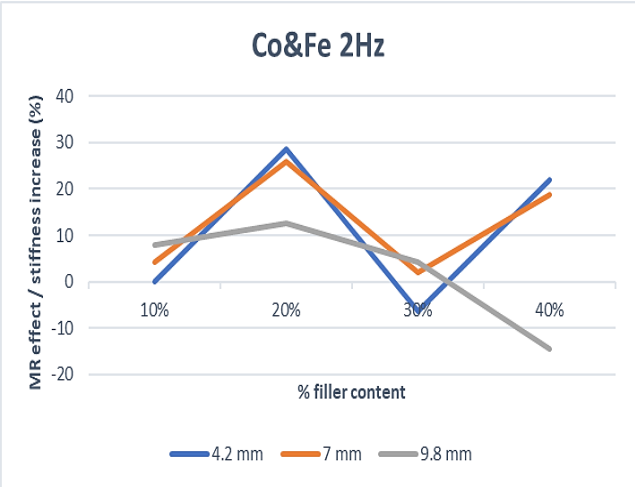

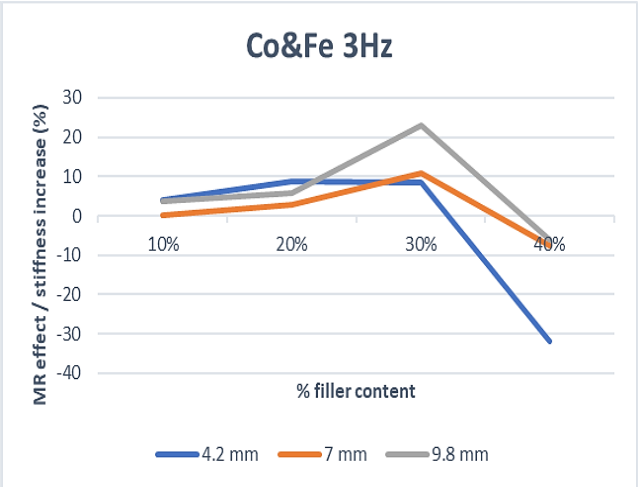

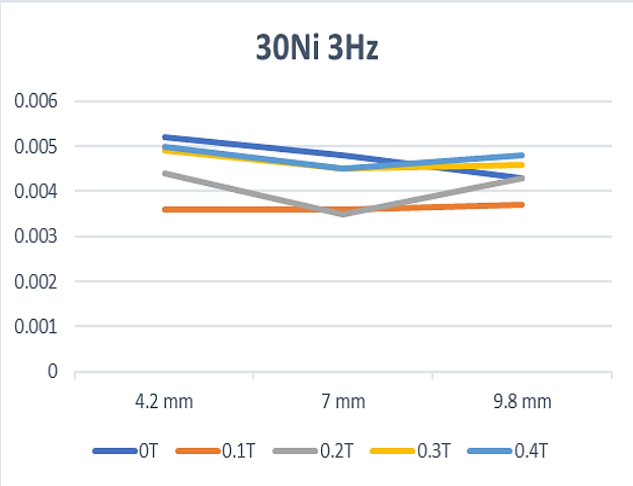
30Ni 3Hz
0.006
0.005
0.004
0.003
0.002
0.001
0
4.2 mm
7 mm
9.8 mm
0T
0.1T
0.2T
0.3T
0.4T

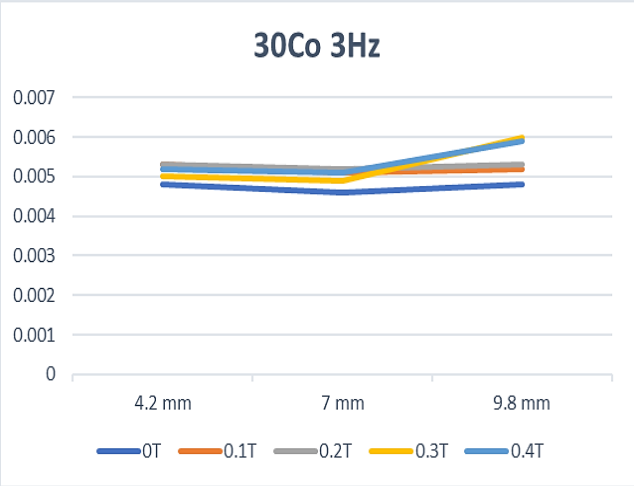
30Co 3Hz
0.007
0.006
0.005
0.004
0.003
0.002
0.001
0
4.2 mm
7 mm
9.8 mm
0T
0.1T
0.2T
0.3T
0.4T

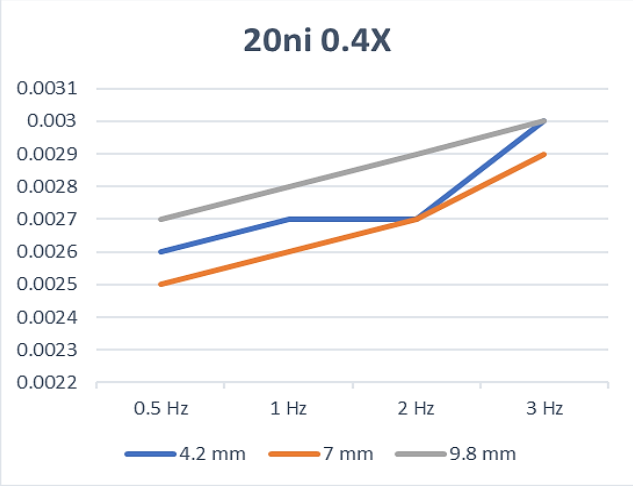
20ni 0.4X
0.0031
0.003
0.0029
0.0028
0.0027
0.0026
0.0025
0.0024
0.0023
0.0022
0.5 Hz
1 Hz
2 Hz
3 Hz
4.2 mm
7 mm
9.8 mm

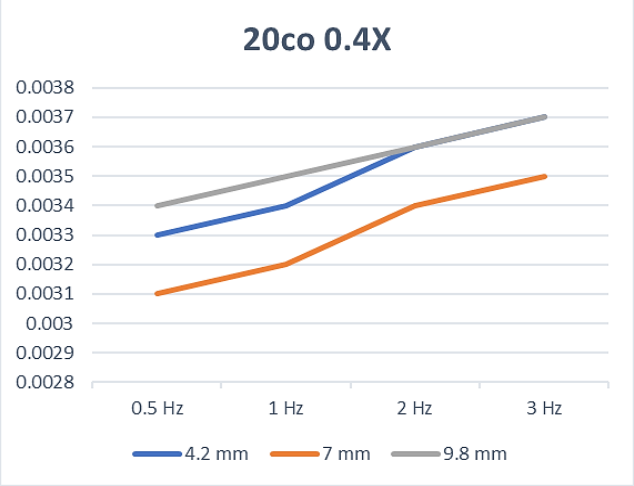
20co 0.4X
0.0038
0.0037
0.0036
0.0035
0.0034
0.0033
0.0032
0.0031
0.003
0.0029
0.0028
0.5 Hz
1 Hz
2 Hz
3 Hz
4.2 mm
7 mm
9.8 mm

Effect of frequency, amplitude w.r.t. filler content

Table 3 MR effect calculations for 20Ni-Fe and 20Co-Fe

			MR effect			
sample	freq	amp	k at X0	k at X0.4	%increase	max
20ni	0.5	4.2	0.0022	0.0026	18.18182	25
	1	4.2	0.0023	0.0027	17.3913	
	2	4.2	0.0024	0.0027	12.5	
	3	4.2	0.0024	0.003	25	
	5	4.2	0.0026	0.0029	11.53846	
	0.5	7	0.0022	0.0025	13.63636	
	1	7	0.0023	0.0026	13.04348	
	2	7	0.0024	0.0027	12.5	
	3	7	0.0024	0.0029	20.83333	
	0.5	9.8	0.0024	0.0027	12.5	
	1	9.8	0.0025	0.0028	12	
	2	9.8	0.0026	0.0029	11.53846	
	3	9.8	0.0024	0.003	25	
20co	0.5	4.2	0.003	0.0033	10	30.76923
	1	4.2	0.0026	0.0034	30.76923	
	2	4.2	0.0028	0.0036	28.57143	
	3	4.2	0.0034	0.0037	8.823529	
	5	4.2	0.0029	0.0037	27.58621	
	0.5	7	0.003	0.0031	3.333333	
	1	7	0.0027	0.0032	18.51852	
	2	7	0.0027	0.0034	25.92593	
	3	7	0.0034	0.0035	2.941176	
	0.5	9.8	0.0034	0.0034	0	
	1	9.8	0.0029	0.0035	20.68966	
	2	9.8	0.0032	0.0036	12.5	
	3	9.8	0.0035	0.0037	5.714286	

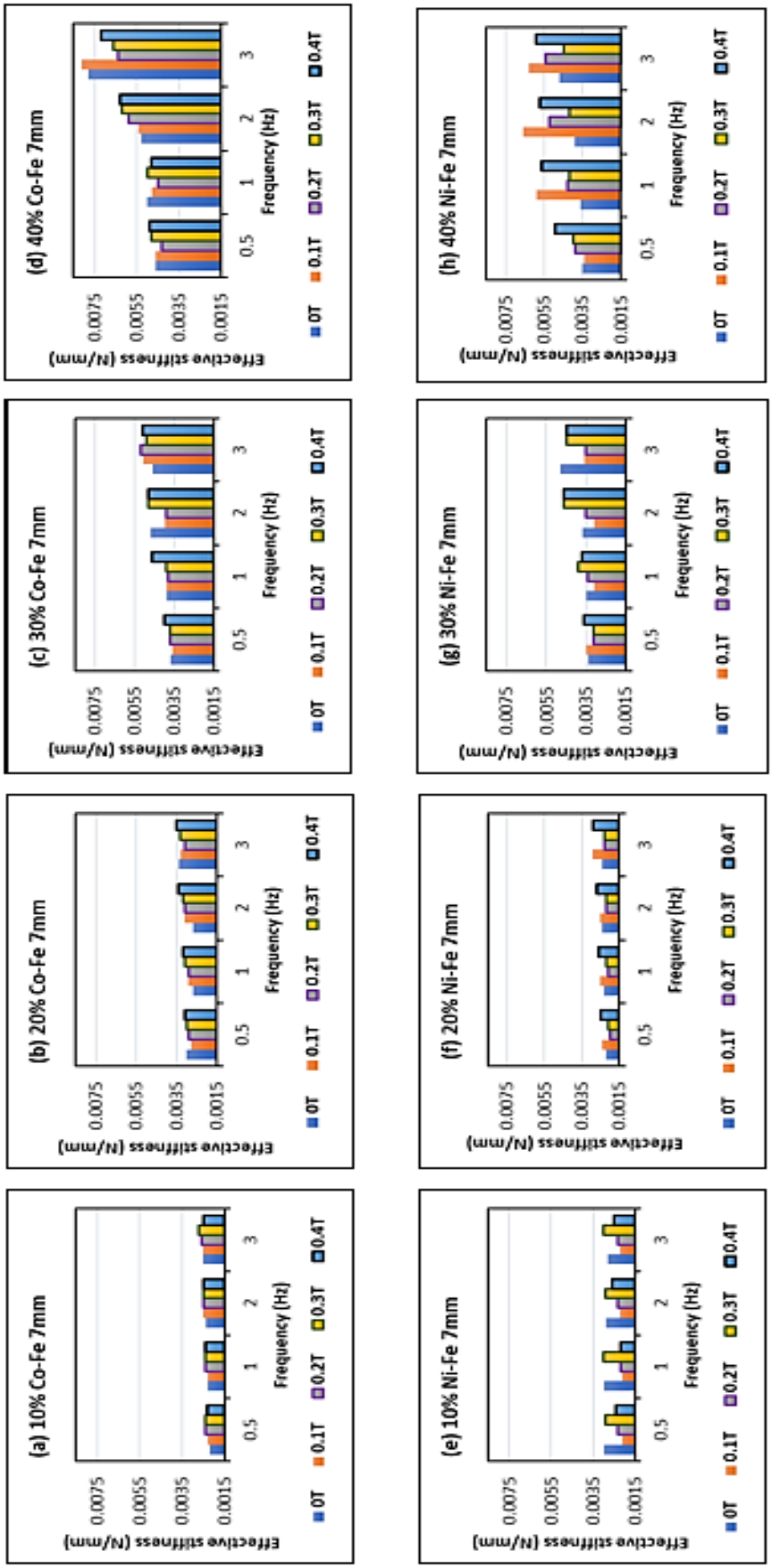

Effect of filler content on effective stiffness

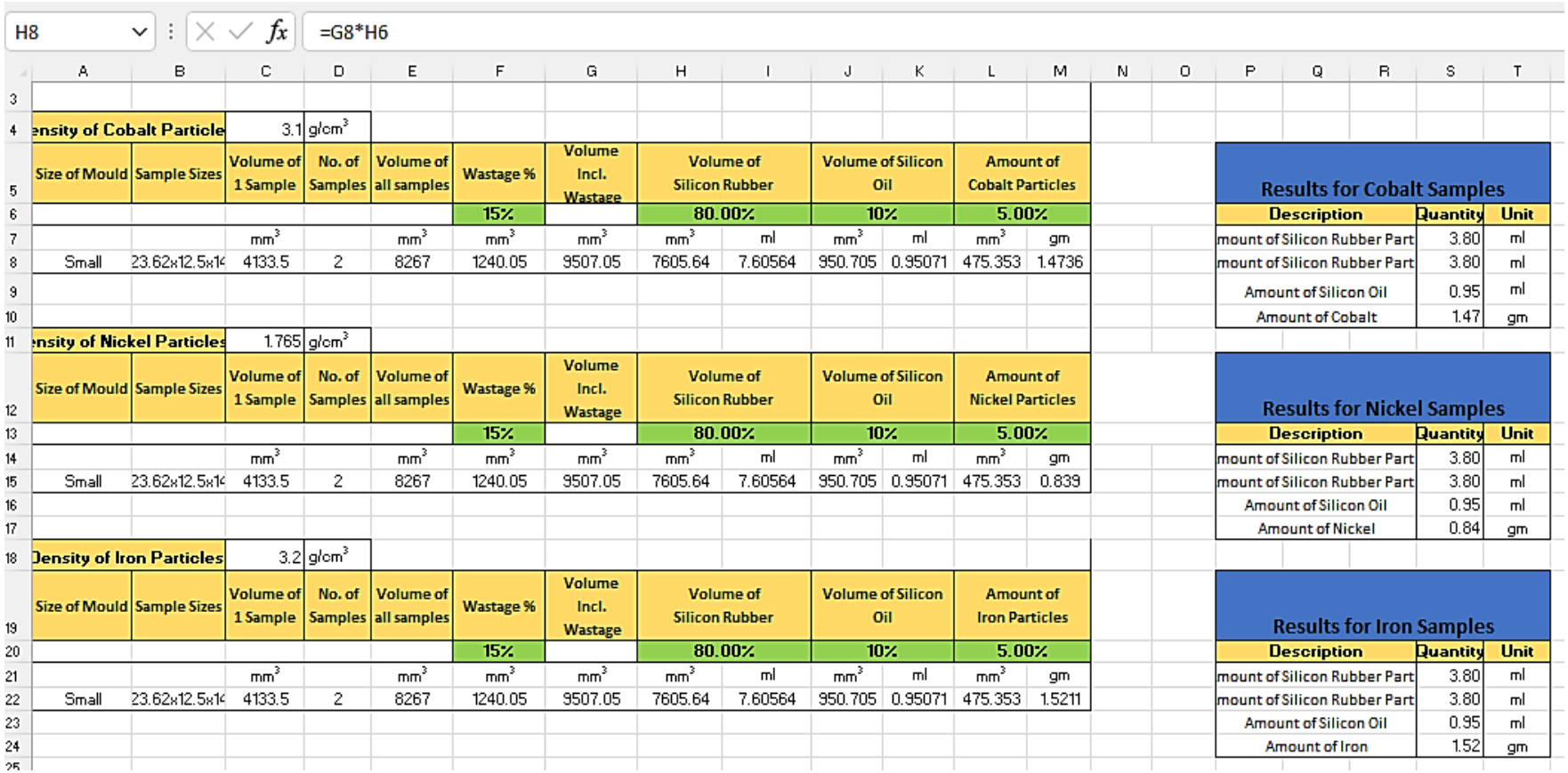

H8 =G8*H6

	A	B	C	D	E	F	G	H	I	J	K	L	M
3													
4	ensity of Cobalt Particle		3.1	g/cm³									
5	Size of Mould	Sample Sizes	Volume of 1 Sample	No. of Samples	Volume of all samples	Wastage %	Volume Incl. Wastage	Volume of Silicon Rubber		Volume of Silicon Oil		Amount of Cobalt Particles	
6						15%		80.00%		10%		5.00%	
7			mm³		mm³	mm³	mm³	mm³	ml	mm³	ml	mm³	gm
8	Small	23.62x12.5x1	4133.5	2	8267	1240.05	9507.05	7605.64	7.60564	950.705	0.95071	475.353	1.4736
9													
10													
11	ensity of Nickel Particles		1.765	g/cm³									
12	Size of Mould	Sample Sizes	Volume of 1 Sample	No. of Samples	Volume of all samples	Wastage %	Volume Incl. Wastage	Volume of Silicon Rubber		Volume of Silicon Oil		Amount of Nickel Particles	
13						15%		80.00%		10%		5.00%	
14			mm³		mm³	mm³	mm³	mm³	ml	mm³	ml	mm³	gm
15	Small	23.62x12.5x1	4133.5	2	8267	1240.05	9507.05	7605.64	7.60564	950.705	0.95071	475.353	0.839
16													
17													
18	Density of Iron Particles		3.2	g/cm³									
19	Size of Mould	Sample Sizes	Volume of 1 Sample	No. of Samples	Volume of all samples	Wastage %	Volume Incl. Wastage	Volume of Silicon Rubber		Volume of Silicon Oil		Amount of Iron Particles	
20						15%		80.00%		10%		5.00%	
21			mm³		mm³	mm³	mm³	mm³	ml	mm³	ml	mm³	gm
22	Small	23.62x12.5x1	4133.5	2	8267	1240.05	9507.05	7605.64	7.60564	950.705	0.95071	475.353	1.5211
23													
24													

Results for Cobalt Samples		
Description	Quantity	Unit
mount of Silicon Rubber Part	3.80	ml
mount of Silicon Rubber Part	3.80	ml
Amount of Silicon Oil	0.95	ml
Amount of Cobalt	1.47	gm

Results for Nickel Samples		
Description	Quantity	Unit
mount of Silicon Rubber Part	3.80	ml
mount of Silicon Rubber Part	3.80	ml
Amount of Silicon Oil	0.95	ml
Amount of Nickel	0.84	gm

Results for Iron Samples		
Description	Quantity	Unit
mount of Silicon Rubber Part	3.80	ml
mount of Silicon Rubber Part	3.80	ml
Amount of Silicon Oil	0.95	ml
Amount of Iron	1.52	gm

Sample proportions